

Optimizing COP of a Direct Fired Double Effect Absorption
Chiller in a Pharmaceutical Plant by employing AI Based
Data Driven Model.



Author

Hammad Pervez

NUST Regn No. 00000318874

Supervisor: Professor Dr. Khurram Kamal

Co-Supervisor : Professor Dr. Tahir Abdul Ratlamwala

DEPARTMENT OF ENGINEERING SCIENCES
PAKISTAN NAVY ENGINEERING COLLEGE (PNEC)

**NATIONAL UNIVERSITY OF SCIENCES AND TECHNOLOGY
(NUST)
ISLAMABAD**

AUGUST 2023

Optimizing COP of a Direct Fired Double Effect Absorption
Chiller in a Pharmaceutical Plant by employing AI Based
Data Driven Model.

Author

Hammad Pervez

Registration Number

00000318874

A thesis submitted in partial fulfillment of the requirements for the degree of
MS in Mechanical Engineering

Thesis Supervisor: Professor Dr. Khurram Kamal

Thesis Co-Supervisor: Professor Dr. Tahir Abdul Ratlamwala

Thesis Supervisor's Signature: _____



DEPARTMENT OF ENGINEERING SCIENCES
PAKISTAN NAVY ENGINEERING COLLEGE (PNEC)

**NATIONAL UNIVERSITY OF SCIENCES AND TECHNOLOGY
(NUST)
ISLAMABAD**

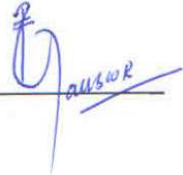

AUGUST 2023

National University of Sciences and Technology

MASTER'S THESIS WORK

We hereby recommend that the dissertation prepared under our supervision by: (Student Name & Regn No.) HAMMAD PERVEZ (00000318874) Titled: "OPTIMIZING COP OF A DIRECT FIRED DOUBLE EFFECT ABSORPTION CHILLER IN A PHARMACEUTICAL PLANT BY EMPLOYING AI BASED DATA DRIVEN MODEL" be accepted in partial fulfillment of the requirements for the award of MS (Mechanical) degree and awarded grade "B" (initial). *Khur*


Examination Committee Members

- | | |
|---|--|
| 1. Name: <u>DR ASIF MANSOOR</u> | Signature:  |
| 2. Name: <u>MR KHURRAM JAMAL HASHMI</u> | Signature: <u>K. J. Hashmi</u> |
| 3. Name: <u>MS SIDRA ZAHID</u> | Signature:  |

Supervisor's name: DR KHURRAM KAMAL Signature: 

CO-Supervisor's name: DR TAHIR ABDUL HUSSAIN RATLAMWALA Signature: 

Date: 25/08/2023


 DR TAHIR ABDUL HUSSAIN RATLAMWALA
 Head of Department
 Commander Pakistan Navy
 Dean Engineering Sciences
 NUST-PNEC

25/08/23
Date

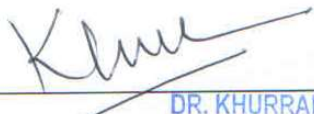
COUNTERSIGNED


Date: 25/08/23

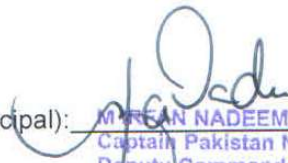

 MIRFAN NADEEM
 Captain, Pakistan Navy
 Deputy Commandant
 PNS JAUHAR

THESIS ACCEPTANCE CERTIFICATE

Certified that final copy of MS thesis written by HAMMAD PERVEZ (00000318874), of NUST - PNEC has been vetted by undersigned, found complete in all respects as per NUST Statues/Regulations, is free of plagiarism, errors, and mistakes and is accepted as partial fulfillment for award of MS degree. It is further certified that necessary amendments as pointed out by GEC members of the scholar have also been incorporated in the said thesis

Signature: 
Name of Supervisor: DR. KHURRAM KAMAL
e Professor
NUST-PNEC Karachi
Date: _____

Signature (HOD): 
DR. MUNTAZIR ABBAS
Commander Pakistan Navy
Head Engineering Sciences
NUST-PNEC
Date: 25/08/23

Signature (Dean/Principal): 
M. REHAN NADEEM
Captain Pakistan Navy
Deputy Commandant
PNS JAUHAR
Date: 25/08/23

Declaration

I certify that this research work titled “*Optimizing COP of a Direct Fired Double Effect Absorption Chiller in a Pharmaceutical Plant by employing AI Based Data Driven Model.*” is my own work. The work has not been presented elsewhere for assessment. The material that has been used from other sources it has been properly acknowledged / referred.



Signature of Student

Hammad Pervez
00000318874

Plagiarism Certificate (Turnitin Report)

This thesis has been checked for Plagiarism. Turnitin report endorsed by Supervisor is attached.



Signature of Student
Hammad Pervez

Registration Number
00000318874



Signature of Supervisor

Language Correctness Certificate

This thesis has been read by an English expert and is free of typing, syntax, grammatical and spelling mistakes. Thesis is also according to the format given by the university.

A handwritten signature in blue ink, appearing to read 'H. Pervez', written on a light-colored rectangular background.

Signature of Student

Hammad Pervez
00000318874

A handwritten signature in blue ink, appearing to read 'Khan', written on a light-colored rectangular background.

Signature of Supervisor

Copyright Statement

- Copyright in text of this thesis rests with the student author. Copies (by any process) either in full, or of extracts, may be made only in accordance with instructions given by the author and lodged in the Library of NUST Pakistan Navy Engineering College (NUST-PNEC). Details may be obtained by the Librarian. This page must form part of any such copies made. Further copies (by any process) may not be made without the permission (in writing) of the author.
- The ownership of any intellectual property rights which may be described in this thesis is vested in NUST Pakistan Navy Engineering College, subject to any prior agreement to the contrary, and may not be made available for use by third parties without the written permission of the NUST-PNEC, which will prescribe the terms and conditions of any such agreement.
- Further information on the conditions under which disclosures and exploitation may take place is available from the Library of NUST Pakistan Navy Engineering College, Karachi.

Acknowledgement

In the name of Allah, the Most Gracious, the Most Merciful.

Praise be to Allah, the Lord of all worlds, and peace and blessings be upon His Messenger, Prophet Muhammad (peace be upon him).

I am profoundly grateful to Allah, the Almighty, for granting me the strength, wisdom, and guidance throughout my journey in completing this thesis. Without His boundless mercy and blessings, this accomplishment would not have been possible.

I extend my heartfelt gratitude to my supervisor Dr Khurram Kamal and Co-Supervisor Dr Tahir Abdul Ratlamwala whose support, encouragement, and invaluable insights have been instrumental in shaping this work. Their dedication and belief in my abilities have been a constant source of motivation.

I am thankful to my family for their unwavering love, prayers, and unwavering belief in me. Their continuous support and understanding have been my pillar of strength.

I am also indebted to my friends, colleagues and the Management Staff at FND, namely Mr. Fahad Abdullah and Mr. Syed Tanveer for their encouragement, assistance, and constructive feedback during this research endeavour. Their contributions have enriched my work and made it more comprehensive

Table of Contents

Declaration.....	v
Plagiarism Certificate (Turnitin Report).....	vi
Language Correctness Certificate	vii
Copyright Statement	viii
Acknowledgement	ix
Table of Contents.....	x
List of Figures	xii
List of Tables	xiii
Abstract.....	xvii
Chapter 1. Introduction.....	1
1.1. Introduction	1
1.1.1. Some of the key advantages of using Absorption chillers are:	3
1.1.2. Disadvantages of Absorption chillers:	3
1.2. Purpose of the Thesis:	4
1.3. Research Objective:.....	5
1.4. Machine Learning and Artificial Neural Networks:	5
1.5. Working Principle of Absorption Chillers	7
1.5.1. The Process of Absorption.....	7
1.5.2. Fundamental Absorption Cycle	8
1.6 Organization of Thesis:.....	9
Chapter 2. Literature Review.....	11
2.1. Performance Enhancement of Absorption Chillers.....	11
2.2. Optimization of Absorption Chiller	16
2.3. Thermodynamic Analysis of Absorption Chiller:	20
2.4. Application of ANN for Absorption Refrigeration Systems:.....	25

2.4.1. Applications	29
2.5. Machine Learning Algorithms employed for prediction of COP for Absorption Chillers:.....	30
Chapter 3. System Description	34
3.1. System Description	34
3.2. Working Principle:	34
3.3. Specifications of the Proposed System	37
3.3.1. Purge System	38
3.3.2. Benefits of Purging:	39
3.4. Crystallization	39
3.5. Thermodynamic Analysis of the DEAC System:	41
3.5.1. General Equations:.....	41
3.5.2. Heat-Transfer-Equation:	42
3.5.3. Equations for Heat Exchangers:.....	45
3.6. Component wise break down of mass balance, energy balance and Exergy Destruction:.....	46
Chapter 4. Overview of Machine Learning Methods	52
4.1. Overview of Machine Learning Models & ANN Algorithms:	52
4.1.1. Artificial Neural Networks:	55
4.1.2. Components of ANN:	55
4.1.3. Backpropagation Neural Network [41, 42]:.....	57
4.1.4. Proposed Algorithm for prediction of COP:.....	60
Chapter 5. Results and Discussions	62
5.1. Energy, Exergy and Exergoeconomic analysis:.....	62
5.2. Exergoeconomic Analysis:.....	67
5.3. Validation of Predictive Results with EES model and Actual Values:.....	Error!
Bookmark not defined.	
Chapter 6. Conclusion & Future Work.....	72

6.1. Conclusion.....	72
6.2. Future Work	73
Chapter 7. References.....	75

List of Figures

Figure 1.1: Absorption Chiller Market by Region (Adapted from [7]).....	1
Figure 1.2: Energy Consumption Distribution in an office building (Adapted from[6])	2
Figure 2.1: Major Approaches for Improving the Energy Performance for a VAC System...	11
Figure 2.2:Absorption cycle types and COP-Comparison.....	12
Figure 2.3:Radial Biased Function (image released as public domain [23]).....	26
Figure 2.4:multi-layer feed forward (image released as public domain [23]).....	27
Figure 2.5:Generalized regression neural networks (image released as public domain [24]).	28
Figure 2.6:Adaptive neuro fuzzy systems (image released as public domain [25])	28
Figure 2.7:Process flowchart of Modelling ANN(Adapted from [22])	29
Figure 3.1:Duhring Plot Parallel flow DEAC (Adapted from [29])	35
Figure 3.2: Schematic of Parallel Flow DEAC (Adapted from [30]).....	35
Figure 3.3:OEM Process flow of the Proposed DEAC System (available to public domain [42])	37
Figure 3.4: Temperature Vs Pressure Plot Indicating DEAC Parallel flow Thermodynamics above Crystallization line (adapted from [27]).....	39
Figure 4.1:Machine Learning (Adapted from [37]).....	52
Figure 4.2: Structure of a Neuron(available to public domain [46])	55
Figure 4.3:Types of Neural Networks (available to public domain [48]).....	57
Figure 4.4:Process Flowchart of BPNN to Predict COP of DEAC System	61
Figure 5.1: Tgen vs Exergetic Efficiency	66
Figure 5.2: Tgen vs COP	66
Figure 5.3:Optimal Neural Network Architecture for COP Prediction of DEAC (Adapted from [28]).....	68

List of Tables

Table 1: Common properties of fluids-Behaviour	7
Table 2: Max and Min Standard Deviation.....	32
Table 3: Key specifications of the actual DEAC System	37
Table 4: Component wise break down of mass balance, energy balance and Exergy Destruction:.....	46
Table 5: Theoretical COP Calculation Parameters.	50
Table 6: input values used for determination of the Enthalpies and subsequent Exergy	63
Table 7: EES model Energy calculation	64
Table 8: EES Model Exergy calculations	65
Table 9: Results of Iterations Summarized.....	69
Table 10: COP Comparison of Actual vs. Predicted vs. EES model	Error! Bookmark not defined.

Nomenclature

\dot{Q}	Heat Rate (KW)
\dot{W}	Work Rate (KW)
\dot{m}	Mass Flow Rate(Kg/s)
h	Enthalpy
A	Heat Transfer Surface Area
$\dot{E}D$	Exergy Destruction
\dot{C}_{cool}	Cost of Cooling
V	Volumetric Flow Rate (m ³ /s)
T	Temperatures (°C)
w	Weight Vector
\hat{y}_i	Predicted Data Point
X	Concentration (%)
\dot{Z}_{eq}	Total Cost of Proposed System
R^2	Regression

Subscript

e	Evaporator
g	Generator
p	Pump
0	Conditions at initial/ambient
i	Initial
f	Final
CWR/CWS	Cooling Water Return/Supply
$CHWR/CHWS$	Chilled Water Return/Supply
HG	High Generator
h	Hidden
o	Output

Greek Letters

θ	Bias
h	Enthalpy (KJ/Kg)
s	Entropy (KJ/Kg.K)
η	Thermal Efficiency
ΔT_{LMTD}	Log Mean Temperature Difference
δ	Output Unit Error
α	Learning Rate
λ	Gas Consumption Rate (Nm ³ /hr)

Acronyms

BPNN	Back Propagation Neural network
MSE	Mean Squared Error
FFNN	Feed Forward Neural Network
R ²	Coefficient of Determination
RMSE	Root Mean Squared Error
HVAC	Heating Ventilation & Air Conditioning
VRF	Variable Refrigerant Flow
ASHRAE	American Society for Heating, Refrigeration and Air Conditioning Engineers
LiBr	Lithium Bromide
RH	Relative Humidity
DB	Dry Bulb Temperature
EES	Engineering Equation Solver
GAX/ AGX	Generator-Absorber Heat Exchanger
GNA	Adjusted Gordon-Ng model Adjusted Gordon-Ng model
MPR	Multivariable Polynomial Model

HPG/HTG	High Pressure/Temperature Generator
LPG/LG	Low Pressure Generator
HTX	High Temperature Solution Heat Exchanger
LTX	Low Temperature Solution Heat Exchanger
ARS	Absorption Refrigeration System
PCA	Principal Component Analysis
BMS	Building Management System
ECOP	Energy Coefficient of Performance
EDR	Exergy Destruction Rate
GA	Genetic Algorithm
MLFFN/MLNN	Multi Layered Feed Forward Neural Network
RACHP	Refrigeration, Air Conditioners and Heat Pumps
GRNN	General Regression Neural Network
BPFFN	Back Propagation Feedforward Neural Network
ANFIS	Adaptive Neuro-Fuzzy Inference System
LM	Levenberg-Marquardt
BR	Bayesian Regularization
MDP	Markov Decision Process
USTR	Unites States Ton Rate
USGPM	United States Gallons per minute
NCG	Non Condensable Gases
ML	Machine Learning

Abstract

An Absorption Chiller stands out as a promising technology, particularly in regions where consistent power availability cannot be guaranteed. It boasts versatility in being operable with various fuel sources, including waste heat, natural gas, biomass, and solar energy. Notably, its environmental impact is commendable: An Absorption Chiller using the LiBr-H₂O combination, with water as the refrigerant, has no Global Warming Potential (GWP) and no Ozone Depletion Potential (ODP). This is a significant advancement compared to Electric Chillers using CFCs.

Historically, predicting the Coefficient of Performance (COP) has often relied on system simulation. However, this method's effectiveness hinges on constructing an accurate system model through component-level modelling, a process prone to time-consuming complexity and convergence challenges due to oversimplification of the inherently nonlinear problem. An alternative approach garnering interest is system-based Artificial Neural Network (ANN) modelling. In this study, Back Propagation Neural Network (BPNN) and Feed Forward Neural Network were used to predict the COP. Training these networks with data from an operational pharmaceutical plant in Karachi, Pakistan, allowed for prediction validation via benchmarking against an EES thermodynamic model—a trusted tool for precise thermodynamic evaluations.

The input dataset for the Feed Forward BPNN Learning Algorithm included variables like Chilled Water Supply Temperature, Chilled Water Return Temperature, Cooling Water Supply Temperature, Cooling Water Return Temperature, and Gas Consumption at the Burner Inlet. Through a comprehensive energy analysis, predicted results were compared to actual data. Encouragingly, the study shows that the FFBPNN method provided highly accurate predictions of absorption chiller performance, supported by a strong correlation indicated by a high R-squared value approaching 1. The neural network predictions closely matched actual COP values within a $\pm 5\%$ margin of error. Additionally, the study extended to analysing a Double Effect Absorption Chiller using an EES-based thermodynamic model

Keywords: BPNN, Energy, Exergy, Absorption Chiller, Parallel Flow, COP, EES, MATLAB

Chapter 1. Introduction

1.1. Introduction

HVAC systems contribute to 12% of global energy demand worldwide which in turn produces 2 billion tons of CO₂ [1, 3]. Furthermore, it consumes of up to 40% [1,2] of energy in Commercial, Residential and Industrial Buildings. With a projected CAGR of 6.6% of the HVAC Global Market by 2026[2], the need to curb Carbon emissions, provide a sustainable future and avoid a paradoxical cycle of rising global temperatures leading to increased HVAC demand is of great importance. The Figure 1.1 below the market growth rate in different regions of the world.

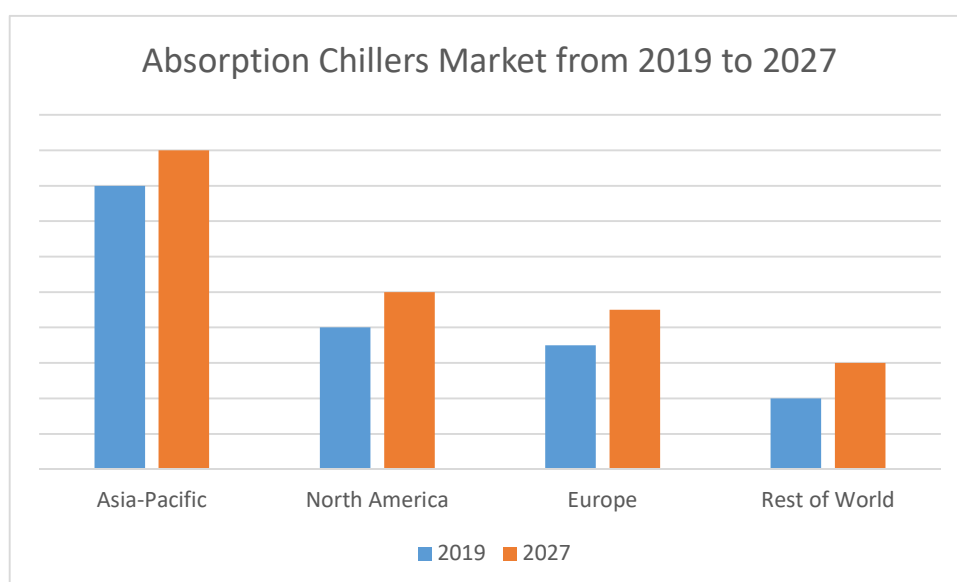


Figure 1.1: Absorption Chiller Market by Region (Adapted from [7])

At present there are several technologies in the HVAC space that constitute 40% of energy consumption in a typical building. Fans consume the most energy standing at 34% followed by cooling equipment such as chillers and packaged units at 27%, then heating equipment stands at 17% with Pumps and Cooling Towers forming as associative equipment for the above Heating and Cooling machines rounding up the energy mix at 16% and 6%[5,7]. Figure below shows the energy consumption distribution in pie chart.

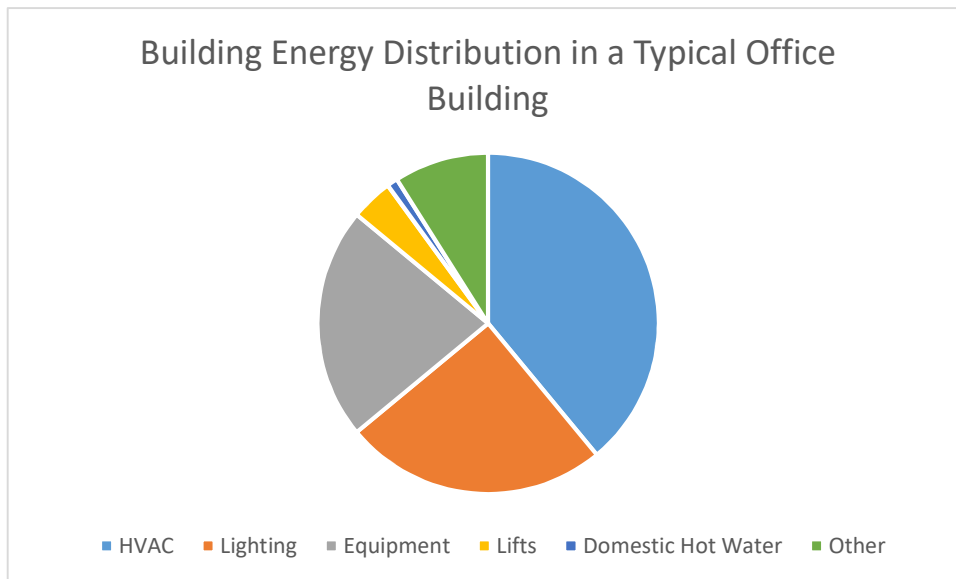


Figure 1.2: Energy Consumption Distribution in an office building (Adapted from[6])

In addition, of the 27% energy consumed, approximately 70% is made up by refrigerant based cooling equipment such as Packaged Rooftop Units, Split Air Conditioners, VRF based Room Air Coolers etc[5,7]. The reason could understandably be the ease of installation, maintenance and intelligent controls makes it an attractive prospect especially when compared to the Initial Capital cost of Chilled water-based Cooling Systems. On the other hand, however as per ASHRAE, median life of these systems are far lesser than Chilled water-based systems so they will continuously be required to be replaced. The operational cost and resultant capital cost in retrospect will eventually equal or exceed that of Chilled Water based systems in the long run.

In contrast, Cooling based on provision chilled water-based systems constitutes to around 28% mostly based on Electrically Driven Chillers. This profoundly impacts the energy mix and leads to high dependency on fossil fuels to provide sufficient electricity for operation.

Thus, we need to look at Renewable technologies in this space to mitigate adverse impacts on the environment. One such technology has been in existence for decades, however despite it serving as a viable alternative to Electric Operated Chillers, never really has gained much traction until recent years. The Global Market for Absorption Chillers stands at approximately 1.5 billion USD and will reach to 2.4 billion USD until 2032[3,4]. Absorption chillers barely contributes to 2% of the energy which means it serves as viable alternative and the only renewable technology fundamentally [1].

1.1.1. Some of the key advantages of using Absorption chillers are:

1. Does not have Electrically Driven Compressor as it operates on the Vapor Absorption cycle. As a result, it possesses the capability to operate using various fuel sources, including residual heat generated by industrial operations, Bagasse, Solar Thermal Energy, Natural Gas, Steam, and more.
2. Lower operating costs due to lesser moving parts. A well-maintained Absorption Chiller can outlast an electrically driven chiller with expected lifetime of above 25 years.
3. Working fluid is free from CFC's which can damage the Ozone layer especially in the case of LiBr-H₂O based Absorption chillers where water acts as the refrigerant. Thus, the working substance does not contribute to Global Warming Potential (GWP) or Ozone Depletion Potential (ODP).
4. Quieter Operation due to absence of compressor. This can reduce noise pollution especially in commercial and residential buildings.
5. There is no Start and Stop operation cycling loss during which electrically driven chillers are notorious for producing excessive waste heat.
6. Efficient at utilization of Low-grade heat sources. [8]

1.1.2. Disadvantages of Absorption chillers:

1. Higher Capital cost due to use of expensive components in manufacturing and LiBr can sway the decision towards Electrically Driven Chillers.
2. Cost of and Complexity of Maintenance is significantly higher. This is because one of the major drawbacks is the issue of crystallization of the LiBr salt when it's the machine is operated at near the saturation temperature of the LiBr Salt which causes it to solidify. This in turn becomes extremely corrosive and significantly impacts the life of the Heat Exchangers within the machine.
3. Absorption chillers are typically larger in size and weight which can make them difficult for shifting operations.
4. They have significantly lower COP than Electrically driven chillers which is one of the major drawbacks of absorption chillers. They are also less efficient at converting energy into heat extraction potential unlike electrically driven chillers.
5. Vacuum Leaks are extremely damaging for an Absorption chiller. Any points of entry of air can cause rapid rate of corrosion when combined with the salt and water[8].

Nevertheless, many of the modern Absorption chillers have been incorporated with modern electronic controls and purge systems so any criticality or limiting factors of the Absorption have been nearly eliminated. This has made them more viable with the exception of COP which cannot be matched to that of electrically driven chillers. Nevertheless, numerous research endeavours have sought to improve the Coefficient of Performance (COP) of Absorption Chillers., and this will be explored in detail in Chapter 2.

1.1.3. Major use cases for Absorption Chillers:

2. One of the key applications of an Absorption Chiller is to provide process cooling water for various industrial purposes using waste heat from exhaust/flue gases.
3. They can also be used for application where non-stop cooling or chilled water is required for instance, in sectors like pharmaceuticals, refrigerated storage facilities, data centres, and district energy plants, among others.
4. They can also be used for residential applications due to the nature of low noise during operation especially during night time.
5. It can be used in areas where electricity availability is limited and/or can be expensive.
6. Can be used as standby or backup during enhanced cooling load requirement or act as a failsafe.

Keeping in view of the above applications and the annual growth rate of the absorption chiller market, it would be helpful to investigate and study all the techniques that may enhance the operational ability of the Absorption Chiller. This in turn will help motivate a greater rate of transition towards its use by increasing its efficacy [8].

1.2. Purpose of the Thesis:

With the current advent and rapid development of Machine Learning and Deep Learning methods. One such approach is to employ Artificial Neural Networks and use the Data Driven Model to make intelligent decisions with respect to improving efficiencies by predicting optimal conditions from real time data and then generating control strategies.

Fault diagnosis, prediction and maintenance schedules can be done not just based on the rated life of equipment or as per OEM guidelines but anomalous behaviour from historic data and normal operating patterns especially when integrated with Condition based health monitoring tools. Then, inform the operator before time leading to proactive maintenance rather than reactive maintenance.

Absorption chillers can have varying designs. Also, the manufacturers themselves do not mention the internal working parameters of the absorption chiller. Therefore, it is not possible to predict the internal efficiencies of components. With the help of Neural Networks, we can link the external data provided by the manufacturers with that of the internal data by training it to form nonlinear complex relationships to accurately predict parameters such as COP, energy and exergy using base parameters derived from the operation of the Absorption Chiller.

Additionally, using traditional analytical models to predict COP requires oversimplification and assumptions. With the help of real time datasets being analysed and trained to predict the COP, it can eliminate the assumptions and will be in close proximity the actual COP of the system. There might also be cases where missing data and/or corrupt data may cause issues with regards to operation parameters and prediction of COP. Neural networks can extrapolate from historic data to still make meaningful predictions. This can help to increase energy efficiency and improve fuel savings.

1.3. Research Objective:

- Develop an AI based data driven model and optimize the efficiency of the absorption chiller.
- Conduct an examination that encompasses Exergy, Exergo-economic, and Energy, and analyses of the planned absorption chiller system utilizing the EES software
- To compare the developed model with simulation results.

1.4. Machine Learning and Artificial Neural Networks:

Neural Networks constitute the foundational framework of Deep Learning, which falls under the umbrella of Machine Learning. They are structured with layers of interconnected nodes, akin to algorithms mimicking human brain functionality. These networks recognize data patterns through sequential layers, comprising an input layer, one or more hidden layers, and an output layer. Within each layer, distinct nerve cell executes computations on input data, relaying outcomes to subsequent layers for further analysis.

Neural connections are allocated weights according to user-defined parameter priorities. During the learning phase, as the network is exposed to input data and corresponding output labels, these weights are adjusted. The aim is to reduce the difference or variance between the network's predictions and the target output labels. This iterative process is referred to as Backpropagation.

In the context of Artificial Intelligence, Machine Learning serves as a subset. Its core focus lies in crafting models and algorithms these methods empower computers to independently learn from data and enhance their performance progressively, all without the need for explicit programming. The overarching aim of Machine Learning is to empower computers to anticipate future events, identify trends, and execute tasks by leveraging discerned patterns and insights extracted from data.

Machine learning can be categorized into three distinct groups:

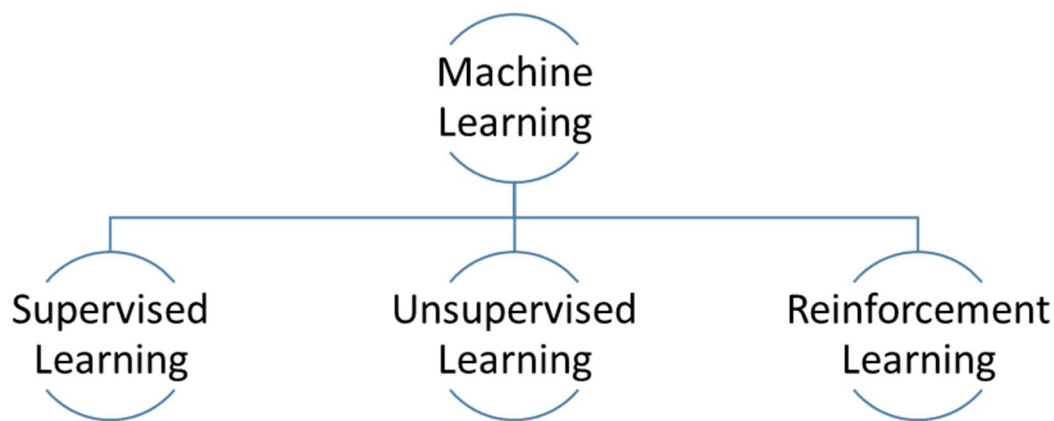


Figure 1.3: Machine Learning Facets

- a. **Supervised Learning:** In this method, input characteristics and associated output (target) values are provided, and the machine learning model is trained on labelled data. In order to be able to predict outcomes from new, unforeseen data, the model must first learn to map inputs to outputs.
- b. **Un-supervised Learning:** In unsupervised learning, the model is qualified on data that has not been assigned a label, and its objective is to find structures or patterns in the data. Techniques like dimensionality reduction and clustering are included.
- c. **Reinforcement-learning:** Teaching an agent to engage with its surroundings and gain knowledge from the feedback it receives. In order to maximize cumulative rewards over time, the agent acts in the environment and is rewarded or penalized as a result.

There are many methods and sub classifications which will be further discussed in Chapter 2 and Chapter 4 pertaining to which Neural Networks and what Machine Learning algorithms have been used in the past to estimate certain parameters of an Absorption Chiller and its efficacy while doing so.

1.5. Working Principle of Absorption Chillers

1.5.1. The Process of Absorption

The foundational absorption process unfolds as two distinct fluids, each in differing states, convene within the absorber. Through this interaction, they merge to emerge as a singular phase and state. A defining feature of this process involves the disparate saturation temperatures exhibited by the two fluids. Specifically, one fluid's saturation temperature surpasses that of the other. Within this dynamic, the fluid characterized by the lower saturation temperature undertakes the role of the refrigerant. The selection of this refrigerant is contingent upon both its compatibility with the other fluid and the intended operational environment. Such considerations optimize the absorption process, with outcomes contingent upon the cooling requisites of the application, spanning from standard cooling to Sub-Zero Temperature refrigeration.

Prominent among the fluid pairs employed in absorption processes are LiBr-H₂O and NH₃-H₂O. In the former, water functions as the refrigerant, while ammonia serves this purpose in the latter. LiBr-H₂O finds application in cooling scenarios where temperatures remain above freezing. This choice is substantiated by its commendable Coefficient of Performance (COP), low toxicity, and simplified handling. Conversely, NH₃-H₂O proves indispensable for refrigeration due to ammonia's remarkably low boiling point of -77.7°F.

The subsequent Table 1 enumerates the predominant properties that underpin the efficacy of the aforementioned fluid pairs. It serves as a guide to the extent to which these properties are met by the respective fluid combinations:

Table 1: Common properties of fluids-Behaviour

Properties of Refrigerant Pair	Ammonia/Water	Water/Lithium Bromide
Refrigerant		
Moderate vapor pressure	5	6
Low viscosity	2	2
High latent heat	2	1
Low freezing temperature	1	4
Absorbent		

Low viscosity	2	2
Low vapor pressure	3	1
Mixture		
High affinity between refrigerant and absorbent	2	2
No solid phase	1	4
Low toxicity	3	2

Note: The Numbers represented above are identified as 1-Excellent 2-Good 3-Poor 4-Limited Application 5-Too High 6-Too Low.

1.5.2. Fundamental Absorption Cycle

The operation of an absorption chiller is underpinned by six fundamental subsystems, In this context, the focus is on illustrating a Single Effect Absorption Refrigeration System for clarity

1. **Absorption of Refrigerant:** The cycle commences within the absorber, housing a blend of Lithium Bromide (Absorbent) and Water (Refrigerant). The heated refrigerant from the evaporator mixes with the diluted solution in the absorber.. This merging, which is an exothermic procedure, emits heat to the environment.
2. **Generator:** The potent solution advances to the generator or desorbed. Here, an external heat source like natural gas or steam warms the solution. As a result, the refrigerant separates and vaporizes from the potent solution, emerging as saturated vapor at elevated pressure.
3. **Condenser:** The saturated vapor proceeds to the condenser, interacting with cooling water from the cooling tower. This interaction triggers condensation, Conversion into high-pressure vapor liquid refrigerant as it undergoes the transition, marking a phase change.
4. **Expansion:** The high-pressure liquid refrigerant journeys through an expansion valve, where abrupt pressure alteration causes partial Evaporation during expansion.
5. **Evaporator:** The heated chilled water loop interfaces with the partially vaporized refrigerant in the evaporator. This prompts another phase shift, transforming the refrigerant into a superheated, low-pressure state.

6. **Solution Heat Exchanger:** Typically, The heat exchanger aids in the exchange of thermal energy between the diluted solution returning from the generator and the concentrated solution directed to the generator. This internal exchange doesn't entail phase transition. It optimizes energy utilization, curbing waste heat and reducing generator heat input.

Subsequently, the weakened solution, following the solution heat exchanger, traverses an expansion valve, attaining parity with the absorber's pressure level as a two-phase vapor-liquid solution stream. This cyclical process repeats, constituting the elemental operational cycle for the Single Effect Absorption Chiller.

The preceding discourse provides a high-level glimpse into the functionality of an absorption chiller. This overview lays the groundwork for comprehending the system under scrutiny in the present study.

1.6 Organization of Thesis:

The research work presented in this manuscript adopts a methodical and well-structured approach, wherein each CHAPTER and subsequent section is dedicated to distinct facets of study. The main emphasis of this research centres on the prediction and optimization of COP using Back propagation Neural Network from real time data available. Following which benchmark, it with EES model and that of the real-world COP.

Literature Review: CHAPTER 02 encompasses historical research works that have been carried with respect to enhancing the Absorption Chillers' capability either through novel design or through software-based approaches such as the use of Data Driven Models. Moreover, there were several areas in the past research work which could benefit from ancillary studies forming part of future research.

System Description: CHAPTER 03 discusses the current system under study and the reason for this specific system to be chosen. Further a detailed analysis was also carried to best select the Neural Network to employ on the selected system and residual justification duly stated.

Thermodynamic Analysis: CHAPTER 04 outlines the mass balance, energy balance, irreversibility's using exergetic analysis and finally the Exergoeconomic analysis of the stated system under study. This was done to conform to objectives and verify the results of the EES model.

Results and Discussion: CHAPTER 05 illustrates the outcome of both ML based Model and EES model. These are outcomes are exhibited both through analytical representations as well as in graphical/tabulated forms. To assess the validity and significance of the findings, the results are benchmarked with historical works in the field.

Conclusion: The conclusion of the research, analysis, and experimental findings based on the data gathered throughout the study are presented in the manuscript's CHAPTER 6 . This section highlights the ramifications and importance of the research while summarizing the major findings. It also offers recommendations for future research, detailing possible lines of inquiry and advancement in the area. The conclusion also addresses gaps and restrictions in the current research, highlighting areas that need focus and more research in subsequent studies.

Citations and References: The work follows strict guidelines for citations and references. The document concludes with a complete list of references that includes all the sources consulted during the research. These citations are used to give due credit and recognition to the original authors and works that helped shape the study. Additionally, proper in-text citations are used all throughout the work to provide accurate attributions for particular facts or ideas that were taken from other sources. This permits the verification of claims made in the study and ensures academic integrity, authenticity, and transparency in the depiction of the research.

Chapter 2. Literature Review

2.1. Performance Enhancement of Absorption Chillers

Rasoul Nikbakhti et.al comprehensively reviewed several methods and studies that have improved the Absorption Chiller Technology's' performance and efficiency. The flowchart in Figure 2.1 below summarizes the key areas of the absorption cycle where improvements have been made including reconfiguring the absorption cycle itself.

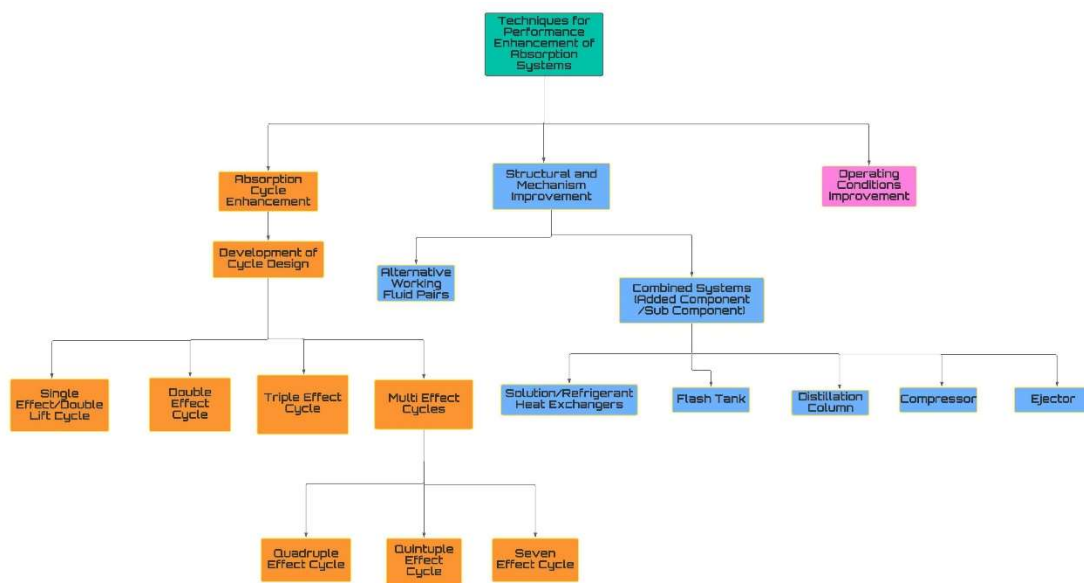


Figure 2.1: Major Approaches for Improving the Energy Performance for a VAC System

The first part of his research focused on cycle improvements which starts from a basic single effect cycle all the way to seven effect cycle.

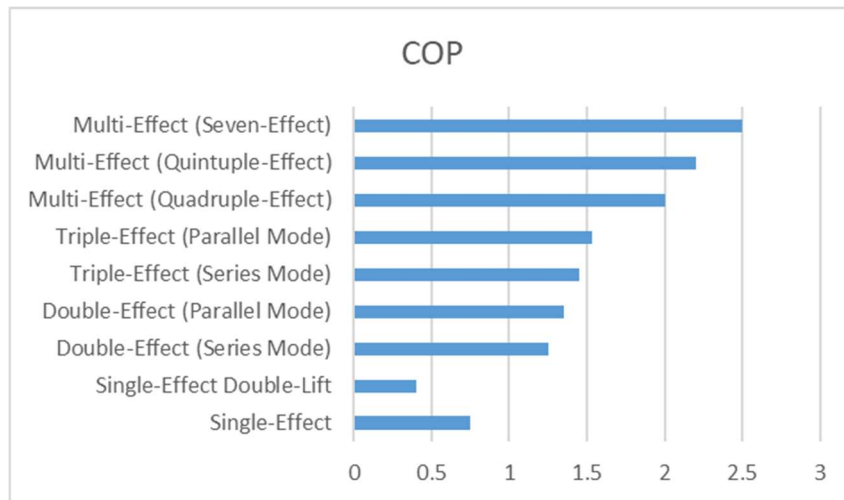


Figure 2.2: Absorption cycle types and COP-Comparison

As indicated in Figure 2.2 above and inferred from existing literature, there exists an unswerving association between the number of stages and the COP (Coefficient of Performance). Amplifying the number of stages yields improved COP values. However, this enhancement comes at a substantial cost, introducing elevated operational intricacies into the cycle. Moreover, the returns on performance become progressively marginal. This escalation in the machine's size is coupled with the requirement for higher generator temperatures in multi-stage cycles to attain heightened COPs. Yet, this is often unattainable given the typical usage scenarios of absorption chillers, primarily designed to leverage low-grade heat sources for cooling.

In the subsequent section of the report, strategies to augment the single-effect absorption cycle are explored, primarily focusing on heat recovery methods, particularly the Generator-Absorber Heat Exchange (GAX) cycles. Among these, the Regeneration cycle, an advanced form of heat recovery, stands out, manifesting a notable 30% performance boost compared to conventional GAX cycles.

Furthermore, fluid pairs like water/sodium hydroxide, water/sulfuric acid, and ammonia/sodium thiocyanate, while possessing untapped potential, have not gained significant market traction. Their limited adoption is attributed to their expensiveness, reliance on specialized equipment, and operation-altering modifications, rendering the Absorption Chiller excessively intricate to maintain and operate. This underscores the continued prominence of Ammonia-Water and Aqueous Lithium Bromide fluid pairs due to their inherent advantages.

The incorporation of sub-components such as Solution Heat Exchangers, Flash Tanks, and Distillation Columns can tangibly enhance the COP without necessitating increased

complexity. Cascade Absorption Compression systems, similarly, hold promise in significantly elevating COP values, approaching those of Vapor Compression Refrigeration systems.

Notably, in contrast to other internal components of the Absorption Chiller, variations in generator temperatures exert a critical influence on the COP. The rule of thumb dictates that higher Generator Temperatures correspond to greater COP values.

Arnas et al. introduced a pioneering Absorption-Chiller system, the solo double-effect absorption-chiller, powered by solar energy. This innovative approach adapts to varying solar energy availability due to seasonal changes. The study recommends a hybrid method, using Single Effect for 50% of peak cooling load and Double Effect for the remaining 50%. This strategy optimizes part-load performance during off-peak cooling demands while harnessing maximal solar energy during peak cooling requirements. Moreover, the Double Effect mode which can run with a higher-grade heat source such as natural gas etc. and becomes a fall back when solar energy is insufficient, thus ensuring consistent and efficient operation. The system contains a total of 7 main components namely:

- a) Chilled-Water Evaporator.
- b) Solution-Absorber.
- c) Special-Temperature-Generator.
- d) Advanced-Condenser.
- e) High-Temperature Generator.
- f) Low-Temperature Generator.
- g) Condenser.

The system can use all the components when it's in Single-Double Effect mode or it can use only the 4 components when in Single effect mode, or 5 components when in Double effect mode. The cooling water flow path is what differentiates the Single-Double effect mode from either of the two individual systems.

Finally, using advanced optimal control strategies to deduce optimal operation points. The COP of the entire Cycle can be improved by 5%.[33]

In 2013, Labus, Jerko, Joan Carles Bruno, and Alberto Crowns embraced an exhaustive examination utilizing different displaying ways to deal with assess the exhibition of little limit retention chillers. Their review incorporates a careful assessment and correlation of clear yet exceptionally exact consistent state models for little limit retention chillers. The models are created in view of carefully assembled trial information from a cutting edge test seat

highlighting a twelve-kW retention chiller. These models hold promising potential for coordination into far reaching displaying and re-enactment instruments, as well as control procedures for cooling frameworks in view of retention chillers. The study includes a complete evaluation of various demonstrating systems for anticipating the exhibition of retention chillers. Four tentatively grounded models were utilized in this unique circumstance:

- Adjusted Gordon-Ng model (GNA)
- Trademark condition model ($\Delta \Delta t'$)
- Multivariable polynomial model (MPR)
- Counterfeit brain network model (ANN)

Each of these models underwent extensive testing using experimental data. The report encompasses various statistical metrics and tests aimed at facilitating the choice of the most appropriate model. The impressive statistical metrics include a coefficient of determination surpassing 0.99 and a coefficient of variation at 5% strongly suggest the feasibility of constructing highly accurate empirical models utilizing solely the input parameters related to external water circuit variables. [16]

In 2010, a conference presentation by Mr. Farshi, L., and Mohand Mahmoudi compared three variants of double-effect-liquid/water absorption-refrigeration-systems. The study aimed to assess and contrast the performance of these three configurations:

Series 2. Parallel 3. Reverse parallel, with similar refrigeration capacity.

A novel set of mathematically streamlined equations has been employed to model the thermal characteristics of Li-Br configurations at equilibrium, enabling the depiction of system performance. Utilizing simulation results, the study delves into the influence of operational factors, encompassing HPG (high-pressure generator), evaporator, condenser, etc., The study assesses crucial metrics including COP (Coefficient of Performance), peak COP, and the ideal HPG temperature for achieving maximum COP. It also delves into the effects of factors like the effectiveness of the solution heat exchanger, pressure differentials (P_{drop1}) between the evaporator and absorber, and (P_{drop2}) between the low-pressure generator (LPG) and the condenser. Furthermore, the impact of introducing low-grade external heat to the LPG on system performance is explored.

The findings furnish insights of value for system planning, management, and configuration evaluation. The research underscores that elevating T_{HPG} (temperature of high-pressure generator) up to a certain threshold enhances COP across all three systems. Beyond this point, the COP exhibits marginal variations with rising T_{HPG} . Notably, decreasing T_{con} ($=T_{abs}$) and/or increasing T_{eva} contributes to lowering the optimal T_{HPG} for maximum COP while elevating both COP and its pinnacle value.

Comparing the three systems, it becomes evident that parallel systems exhibit higher COPs than series systems, akin to the scenario in reverse parallel systems. Among the design parameters, P_{HPG} (pressure at high-pressure generator) assumes critical importance, with proximity to atmospheric pressure being optimal. For series flow setups, P_{HPG} responds favorably to augmented T_{HPG} and T_{con} or reduced T_{eva} . In parallel and antiparallel setups, P_{HPG} is enhanced by lowering T_{eva} and raising both T_{HPG} and T_{con} . Improving the heat exchanger's efficacy as LTE (Low-Temperature Evaporator) leads to a more efficient boost in COP for all three systems.

An important factor is the pressure drop between the evaporator and absorber, as reducing this drop is crucial to maintaining a high COP. Additionally, using the low-pressure generator (LPG) becomes beneficial when there's a source of low-grade waste heat.[8]

In 2011, a comprehensive evaluation of an absorption refrigeration system (ARS) performance was carried out by Myat, A., and co-workers. This evaluation employed entropy generation analysis as a method to assess the system's efficiency and effectiveness... They developed an algebraic model that predicts the absorption cycle's performance during transient conditions, including entropy generation calculations at various heat source temperatures. The dynamic variations in the lithium bromide solution's characteristics, This model also considers properties like concentration, density, vapor pressure, and overall heat transfer coefficients. They employed a genetic algorithm (GA) for optimization, aiming to determine system minimums for varying temperatures for the heat source and the cooling water. They presents entropy generation values for each chiller component at various hot water temperatures, along with simulated parameters for a 35 kW nominal capacity absorption chiller in their study. Their findings suggest the potential for optimizing a network of interconnected heat-sensitive appliances to maximize the conversion of waste heat into valuable outcomes. [32]

In the 2013 study conducted by Xu, Z et al, put forth the idea that a temperature range of 110°C to 140°C for power generation can have a dual positive impact. As the traditional LiBr-water

absorption cycle is known to function at temperatures much greater than, for a single-effect cycle. The researchers introduced an innovative oval LiBr-water-absorption cycle with an Absorber-Generator heat exchanger (AGX). This AGX absorption cycle utilizes condensation heat at high pressures across various temperature ranges, resulting in variable levels of supplementary refrigeration. This innovation leads to a multi-effect (1.n-effect) refrigeration process.

This distinct cycle operates effectively within the temperature spectrum of 85 to 150 degrees Celsius. It encompasses specific temperature parameters: evaporation temperatures of 5 degrees Celsius, absorption temperatures of 35 degrees Celsius, and condensation temperatures of 40 degrees Celsius. Simulation outcomes showcased the oval cycle's capability to function in diverse modes: single-effect mode, single-effect mode with intercooling (for generating temperatures ranging from 85°C to 93°C and 93°C to 140°C, respectively), and double-effect mode (for generating temperatures of 140°C to 150°C). The corresponding Coefficients of Performance (COPs) for these modes are 0.75, 0.75 to 1.08, and 1.08 to 1.25.

Through a comparative analysis against an existing cycle that operates within similar temperature ranges for power generation, the researchers highlighted the superior performance of their proposed cycle. Due to its wide operational range, this cycle also holds promise for utilization with medium-temperature solar collectors in solar cooling applications [35].

In a 2019 study at Universitas Indonesia, Aisyah et al developed an Artificial Neural Network (ANN) model to forecast a solar-driven absorption chiller's performance. They carefully selected input parameters, including temperatures, flow rates, and used Principal-Component-Analysis (PCA) to streamline variables and enhance prediction efficiency. The resultant hybrid model, termed "ANN + PCA," combines the ANN model with the integrated PCA approach. This hybrid model showcases exceptional performance and demonstrates error rates comparable to those of the standard ANN model. More specifically, the ANN + PCA model is configured with 9 neurons in the hidden layer, 6 input variables, and 2 output variables. It manages to achieve a remarkable root mean square error of 0.0145 in predicting the Coefficient of Performance (COP).[36]

2.2. Optimization of Absorption Chiller

In October 2012, Velimir Congradac and Filip Kulic conducted research that validates the effectiveness of employing artificial intelligence methods to enhance the operation of chillers.

Their validation procedure encompassed both a simulated office building model within Energy Plus software and practical experiments conducted in an office building that featured an integrated Building Management System (BMS). Their study's primary aim was to optimize chiller performance using artificial neural networks and genetic algorithms.

The research methodology included training an artificial neural network using data obtained from an actual chiller, which subsequently enabled the creation of accurate chiller models. The study's paper not only establishes a foundational understanding of artificial neural networks but also meticulously outlines the essential principles underpinning their operation. Additionally, the researchers delve into the development of specialized chiller models designed specifically for evaluating the results derived from the evolutionary algorithm, thereby omitting the aspect of age optimization.

Furthermore, the research offers valuable insights into the optimal conditions for implementing the evolutionary algorithm, shedding light on the criteria that yield optimal outcomes in the pursuit of chiller optimization.[11]

Vapor absorption refrigeration systems have gained significant popularity due to their utilization of cost-effective energy sources and environmentally friendly operating fluids. A comprehensive exergy investigation of vapor absorption refrigeration systems, specifically focusing on double-effect parallel flow, direct-fired, and indirect-fired configurations employing lithium bromide-water as the working medium, was conducted by Azhar and Siddiqui. This extensive study involves the parametric optimization of temperatures in key components like the main generator, intermediate generator, and condenser. The findings of this research were presented at a journal conference in the year 2020.

Furthermore, the study employs the Exergetic coefficient of performance (ECOP) and the exergy destruction rate (EDR) as crucial metrics for optimizing the distribution ratio of solutions. By maintaining uniform operational conditions, a comparative analysis is performed between parallel and series flow topologies. The investigation also delves into exploring the impact of temperature differences between the intermediate generator and intermediate condenser on both cycle types.

The results of the research exhibit that the ECOP of the parallel flow DEAC cycle was consistently 3-6% greater than compared to the series flow DEAC cycle. Additionally, the study reveals that the lowest EDR is approximately 4% lower in Parallel flow configuration.

As a valuable resource for design engineers, the research provides optimal specifications for both series and parallel flow cycles.[19]

In 2017, Azhar, M., and Siddiqui, M. A. conducted comprehensive exergy and energy analyses on the double-effect lithium bromide-water vapor absorption cycle with the aim of amplifying the exergetic efficiency and COP in the Low Pressure Generator and the secondary generator/condenser. The key approach involved adjusting temperatures within these components to achieve the optimization. Given the presence of two generators in the Double-Effect Absorption Cycle, the optimization process is carried out in two distinct phases. The study also assesses the influence of varying temperatures in ancillary components, namely the absorber, primary condenser, and evaporator.

The research unveils the optimal conditions required to maximize both COP and exergetic efficiency. This encompasses identifying the ideal temperatures for the primary generator, secondary generator, and condenser, in addition to determining the appropriate LiBr-Salt concentrations within the two generators. To facilitate the replication of the cycle, a dedicated computer software is developed.

The outcomes of the investigation reveal a significant correlation between the main generator temperature (T_g) and both COP and exergetic efficiency. As T_g increases, both COP and exergetic efficiency experience improvements up to a certain threshold value of T_g . Additionally, the study finds that while the COP increases with the rise in evaporator temperature (T_e), the exergetic efficiency experiences a decline. [23]

A Double-Effect Parallel flow Aqueous LiBr Absorption Refrigeration Cycle, was in-depthly evaluated by Bagheri, B. S., et. al in their 2019 research study using intensive exercise-based evaluations. In order to conduct a more thorough investigation, the exergy consumption of each device was estimated. With consideration for the distribution ratio variable, the study used the Golden Section technique to optimise the system's performance for the lowest performance and energy efficiency coefficients. The maximum coefficient of performance (COP) of 1.195 and maximum energy efficiency of 0.225 were achieved at 169.6 °C, the temperature of the high-pressure generator. Employing sophisticated exergy analysis, the study not only identified sources of irreversibility but also distinguishable preventable irreversibility. The analysis revealed that focusing on component efficiency is key for system enhancement due to the significantly higher endogenous portion of exercise destruction compared to the external portion. While inevitable exercise destruction remained larger than the preventable portion, the

study showcased a distinct hierarchy of component significance. Moreover, it demonstrated that the system's overall endogenous exergy destruction exceeded its exogenous counterpart, indicating reduced interdependence between components. Notably, the exogenous preventable energy destruction surpassed the endogenous one in low and high-temperature heat exchangers and expansion valves, suggesting potential reductions in energy destruction by enhancing other components. Further, the sophisticated exergy analysis highlighted that most exergy destruction in system components is endogenous and inevitable, with exceptions in low and high-temperature heat exchangers.[24]

In 2002, Chow, T. T., Zhang, G. Q., Lin, and Song, C. L. conducted a research study that emphasized the optimal utilization of fuel and electricity within a direct-fired absorption chiller system for practical operational purposes. In contrast to earlier research endeavors that primarily focused on localized feedback regulation of control scheme components, this study introduced an innovative system-based control strategy that takes into account the interconnected relationship among the building, the plant, and relevant influencing factors.

Departing from conventional approaches, the research proposed a novel control methodology by combining a neural network (NN) with a genetic algorithm (GA) to achieve the most effective control of an absorption chiller system. In this context, a neural network was employed to represent the inherent properties of the system, utilizing its capacity for pattern recognition and learning from data. Additionally, a genetic algorithm was harnessed as a tool for comprehensive optimization, enabling the system to be fine-tuned for maximum efficiency.

To demonstrate the practical application of this approach, the researchers utilized a commercial absorption unit as their basis. The neural network served as a means to encapsulate the complex system properties, while the genetic algorithm played a pivotal role in facilitating holistic optimization, ensuring that the entire system functions optimally in terms of resource utilization and overall performance. [26]

In the year 2019, a comprehensive investigation was carried out by Park, S., Ahn, K. U., Hwang, S., Choi, S., and Park, C. S., focusing on the integration of hybrid machine learning techniques in enhancing the performance of a turbo chiller system installed within an office building. The study involved a comparison between two distinct modelling approaches: firstly, an artificial neural network (ANN) model, and secondly, a hybrid machine learning model that combined the ANN model with the physical properties of the chiller.

To facilitate this analysis, the researchers employed a Gaussian mixture model to pre-process the observed data. The ANN model was then applied to the chiller's operational data. For the hybrid-machine-learning model, the ANN model was coupled with physics-based regression equations, resulting in a comprehensive hybrid system model.

Notably, the hybrid-system model exhibited impressive predictive capabilities in estimating chiller power consumption. Moreover, this model showcased the advantage of requiring a reduced number of input parameters as compared to the standalone ANN model. Remarkably, both the ANN model and the hybrid-machine-learning model led to comparable energy savings, highlighting the effectiveness of the hybrid approach in achieving accurate predictions while offering potential efficiencies in input data requirements.[27]

Chahartaghi, Golmohammadi, and Shojaei, A. F. investigated two innovative series and parallel flow designs for double-effect lithium bromide-water absorption chillers. They evaluated the influence of numerous crucial factors that affect the coefficient of performance (COP). The study considered components such as heat exchangers, condensers, evaporators, absorbers, and generators. Through the application of energy balance equations, concentration, and mass the systems' performances were assessed under various circumstances, with the constraint of avoiding lithium bromide crystallization. The study explored how temperature and mass flow rate variations in the generator's intake vapor and absorber's inlet water affected cooling capacity, heat transfer rate, and COP. Additionally, two parameters were introduced and their impacts on system functionality were studied based on the mass ratio of the solution splitters. According to the results, the series cycle in high-temperature generators (HTG) displayed greater coefficients of performance (COP) than the parallel cycle up to 150 °C. The COP increased in both cycles with an increase in mass-flow amount of absorber intake water and inlet vapor temperature to HTG. Additionally, the COP exhibited an initial rise, reached a maximum value, and then declined. The study also utilized Genetic Algorithm (GA) optimization to optimize the scheme COP in both parallel and series cycles.[28]

2.3. Thermodynamic Analysis of Absorption Chiller:

Joan Carles Bruno and colleagues conducted a study that investigated and delineated two distinct approaches employing the characteristic equation to describe chiller performance, as originally devised by Hellman and others. This approach was built upon a simple model incorporating energy balances, relationships pertaining to heat and mass transfer characteristics, and the thermophysical properties of working fluids. Among the two

approaches identified, one aimed at streamlining operational characteristics, simplifying them into an algebraic equation.

The proposed method based on the characteristic equation introduced the utilization of an arbitrary temperature function, with parameter fitting conducted through multiple regression techniques. This approach was effectively employed to fit real-world data from both single and double effect absorption chillers. Additionally, the researchers undertook a case study to assess the efficacy of the proposed approach against the conventional practice of using an average coefficient of performance (COP) for comparing the performances of two solar cooling plants equipped with absorption chillers.

The outcomes of this research revealed that the model employing the proposed approach yielded results that closely aligned with actual data, outperforming the use of an average COP. Consequently, this novel approach demonstrates its capability in avoiding the employment of overly simplistic and impractical constant and average COP calculations for chiller cooling production across varying operational conditions. Moreover, it mitigates the necessity for an in-depth domain understanding and the development of intricately complex models to achieve satisfactory outcomes. [13]

Gomri conducted a comparative study applying thermodynamic principles to analyze single and double effect absorption chillers. The study used simulation to explore the impact of operational parameters on key metrics like Coefficient of Performance (COP), thermal loads, exergetic efficiency, and overall exergy change. The results showed an optimal generator temperature, where both systems minimized exergy change, maximized exergetic efficiency, and COP. Parameters included evaporator temperatures ranging from 4°C to 10°C, and condenser and absorber temperatures from 33°C to 39°C.

For single effect chillers, COP ranged from 0.73 to 0.79, with exergetic efficiency between 12.5% and 23.5%. In contrast, the double effect system had a COP between 1.22 and 1.42, with exergetic efficiency from 14.3% to 25.1%. This difference, despite the double effect system's higher COP, may be due to its greater heat source requirements. [14]

Gomri and Hakimi applied second law analysis on a double effect vapor absorption cooler system which uses lithium bromide-water based working pair. The Double Effect Vapor absorption system effectively operates between three pressure states due to the addition of a Low pressure generator and addition of a solution heat exchanger. A new set of

computationally efficient formulas were developed for the evaluating the thermodynamic properties of the Lithium Bromide-Water Solution.

In this study the typically used condenser and absorber cooling water temperatures used were 27°C /32°C and Chilled water temperatures used were 12°C /7°C. The computationally efficient formulas were run through fortran. The output identified key components of the system whereby exergy destruction was found to be the highest. The most exergy was lost through the Absorber, followed by the High Pressure and Temperature Generator (HPG) and Solution Heat Exchanger at High Pressure.

It was found that for this particular system, the best COP and exergetic efficiency that were achieved was when the LPG temperature varied between 78°C and 81 °C and HPG Temperature varied between 125 °C and 135 °C.[15]

Yang, Laura and Volker developed three double effect absorption chiller models. One for parallel flow and two were for series flow. The flows indicating series and parallel are part of a solution circuit that indicates the direction of flow between absorber and the regenerators. All three models were assigned the same cooling capacity (16kW), same set of environmental conditions (Room at 9°C and Environment a 40°C), condensing and regeneration temperatures (160°C from heat source). COP was taken at 5.5. All three models were developed in EES software package. The models were derived based on the Carnot and Reverse Carnot Cycle to form an idealized absorption cycle. The relative mass and energy balances were taken with reasonable assumptions.

The results indicated the following:

- The exergy destruction from the Absorber, High temperature generator and High Temperature Solution Heat Exchanger accounts for nearly 70% of the total exergy destruction.
- The first model where Lithium Bromide-Water Solution flows to the low temperature regenerator first has the highest COP at 1.119. However, the solution temperature was at 77.89°C and at 63.89% mass fraction. When the aqueous lithium bromide phase diagram was reviewed it revealed that this kind of solution is susceptible to crystallization which is not favourable.

Hence, the parallel flow double effect absorption exhibits the ideal and best behaviour with COP at 1.022 and no occurrence of crystallization. [20]

This study encompassed a thermodynamic simulation of a double effect series flow absorption refrigeration system that employed water and lithium bromide as the working fluid pair. The primary objective was to conduct a parametric analysis in order to scrutinize the influence of operating temperatures on multiple aspects, including the heat capacity and exergy destruction of the high-pressure generator (HPG), the coefficient of performance (COP) of the system, and the mass flow rate of three distinct heat sources.

As anticipated, the study found that higher heat source temperatures correlated with increased energy destruction. However, it was observed that the required flow rates of the heat sources decreased accordingly. Notably, the flow rate of hot water needed to be lower compared to that of hot air. The study also demonstrated that elevating the operating temperatures of the HPG led to a reduction in its exergy destruction.

When observing the effects of source temperatures, the results indicated that at the lowest source temperature, there was a decrease of approximately 40% for hot air, 42.8% for steam, and roughly 45.6% for hot water in terms of exergy destruction for the HPG. Similarly, a rise in the operating temperature of the low-pressure generator (LPG) was found to contribute to a decrease in the exergy destruction of the HPG. At the lowest source temperature, the exergy destruction reductions were approximately 41.5% for hot air, 41.8% for steam, and around 42.2% for hot water.

Furthermore, the study revealed that with an increase in the condenser and absorber temperatures, the exergy destruction rate of the HPG also increased. Similarly, a slight increase in the exergy destruction of the HPG was observed when the evaporator temperature was raised.

In order to effectively illustrate the contrasting utilization of various heat sources, the study provided absolute exergy destruction values within the figures associated with each respective heat source. [21]

A study similar to the previous ones was conducted by Kaushik and Arora, focusing on both a single effect system and a series flow double effect system. The outcomes of this study were consistent with those previously observed. For instance, the study confirmed that elevating the generator temperature directly results in an increase in both the Coefficient of Performance (COP) and exergetic efficiency. Notably, the COP of the double effect system exhibited an impressive increase of almost 70% compared to that of the single effect system.

However, the study uncovered critical insights regarding the optimal temperature points and the maximal achievable exergetic efficiency for both systems. Specifically, the maximum exergetic efficiency for a double effect system was found to be around 130°C, while the corresponding value for a single effect system was approximately 80°C. Beyond these optimal points, the exergetic efficiency for both systems experienced a decline.

Moreover, the research highlighted that reducing the absorber temperature led to a corresponding decrease in the optimal generator temperature. This reduction, in turn, had a positive impact by increasing both the COP and exergetic efficiency, with the maximum values for these metrics also being affected positively.

However, the study also underscored that enhancing the evaporator temperature had a contrasting effect. While it led to an increase in the COP, it simultaneously caused a reduction in exergetic efficiency.

Finally, the research deduced that elevating the absorber temperature and pressure drop had a notably adverse impact on both the COP and exergetic efficiency, particularly in the case of double effect systems. This was attributed to the fact that the absorber is where the highest entropy generation occurs within the system.[16]

Tugba and Arzu most recently conducted an energy and exergy analysis of a parallel flow double effect absorption refrigeration system. In much the same manner, their results validated what we have already come to know from previous studies, that a majority of the exergy destruction revolves emanates from the Absorber and High Temperature generator. However, they also explored a new avenue where they identified Unavoidable and Avoidable Exergy Destruction. It was found out that approximately 76% of Exergy destruction was avoidable while nearly 24% of Exergy destruction is avoidable by increasing the value of temperature for HTRG, reducing the absorber temperature and condenser temperature but only up to a certain optimal temperature.[22]

Jianke et. al conducted a comprehensive performance evaluation of Double-Effect Absorption Chiller Systems, examining two distinct configurations: series flow and parallel flow. Both configurations had identical capacities of 400kW and utilized the Lithium Bromide-Water working pair. The report will delve into a detailed explanation of the parallel flow system in CHAPTER 3.

The primary difference between the series flow and parallel flow setups in a Double Effect Absorption Chiller lies in the treatment of the strong solution from the absorber. In the parallel

flow cycle, this solution is divided into two segments. One segment is directed towards the Low Temperature Generator, while the other segment follows the traditional flow convention, akin to the series flow chiller, leading to the High Temperature Generator.

The assessment entailed an Energy and Exergy analysis performed through an empirical model based on energy and mass balance principles. This analysis was undertaken to comprehensively evaluate the performance of the two configurations and to discern their respective strengths and weaknesses.[35]

Overall, the following conclusions were derived from the entire exercise:

Parallel flow Absorption chillers exhibit higher COP and Exergetic efficiency when compared to series flow. The annual operational, however, is 19% greater than of the series flow system.

The Heat Transfer Area of the High Temperature HEX is marginally lower than the one in series flow system. The results showed that the highest exergy destruction in a series flow absorption chiller takes place in the Absorber, however same is not true for parallel flow which shows a slightly higher Exergy destruction percentage at the Low temperature Generator.

It was found after the sensitivity analysis, the parameters that had a profound effect on both the chillers were increase in temperatures at the HTG. However only up to a certain optimum point after which exergetic efficiency starts decreasing. The decrease in Cooling water Inlet Temperature increases energy and exergy performance, while increase in Chilled Water Temperature improves heat transfer, increases COP and economic performance but reduces Exergetic Efficiency.

Lastly the solution allocation ratio which basically refers to the concentration of the strong solution should not go beyond 0.54 due to crystallisation issues. The 0.54 concentration value provides the lowest Cost and Heat transfer Area while keeping within the thermo physical limits of the refrigerant pair.[38]

2.4. Application of ANN for Absorption Refrigeration Systems:

Mohanraj, Jayaraj and Muraleedharan did an extensive study on the applications of ANN in HVAC domain. The conventional approaches to model RACHP (Refrigeration, Air Conditioning and Heat pump) done using complex analytical equations and theoretical assumptions led to inaccuracies and oversimplification which was undesirable. To add to that, real time studies were time consuming and expensive. Use of ANN models has been gaining ground over previous decades in all aspects and certainly now in estimating various parameters

of RACHP systems. Its faster than conventional approaches, due to its ability to extract nonlinear relationships from training data as well as solve multivariable problems without requiring any analytical equations.

Among the most widely network architectures in the field of RACHP are the following:

1. **Radial biased function:** Similar to an MLFFN (Multi-Layer Feedforward Neural Network), this structure encompasses an input layer, a hidden layer, and an output layer. However, a distinctive feature sets it apart: the relationship between the input layer, comprising source nodes, and the hidden layer is conceptual or hypothetical in nature. In contrast, the connection between the hidden layer and the output layer is characterized by weighting. The Gaussian transfer function is applied to process the weighted inputs, while the activation function utilizes radial biased function that operates within the hidden layer. Meanwhile, the output layer utilizes a linear transfer function. This modified structure proves to be more dependable compared to the conventional MLFFN. It not only demonstrates enhanced reliability but also exhibits quicker convergence during training. Moreover, its capacity to yield smaller extrapolation errors outperforms the standard MLFFN.

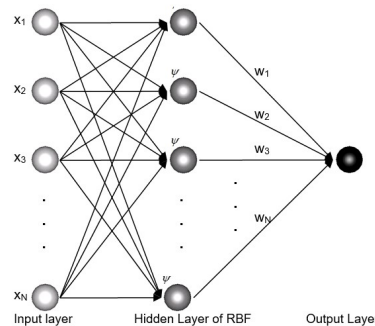


Figure 2.3:Radial Biased Function (image released as public domain [23])

2. **Multi-layer feed forward:** This architecture comprises an input layer, which is followed by one or more hidden layers, and ultimately an output layer. The incorporation of nonlinear transfer functions within this network empowers it to discern and establish correlations spanning both linear and nonlinear connections between input and output vectors. The iterative deployment of the back propagation learning algorithm characterizes the training process for the Multi-Layer Feedforward Neural Network (MLFFN). In this approach, the network is progressively fine-tuned using specific parameters such as the number of neurons in the hidden layer, the momentum factor,

learning rate, and the chosen transfer function. Primarily recognized for its efficacy in the analysis and prediction of RAHCP (Refrigeration, Air Conditioning, and Heat Pump) systems, this architecture is extensively employed for assessing system performance and making predictions within this domain.

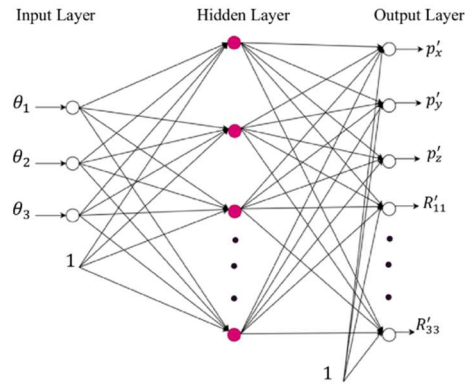


Figure 2.4: multi-layer feed forward (image released as public domain [23])

- Generalized regression neural networks:** Contrasting the prior two architectures, the General Regression Neural Network (GRNN) introduces a distinctive division of the hidden layer into a pattern layer and a summation layer. This model is founded upon principles of nonlinear regression theory. The summation layer itself consists of two distinctive processing units, namely summation units and a solitary division unit. Diverging from the training parameters such as momentum factor and learning rate seen in BPFFN (Back Propagation Feedforward Neural Network), GRNN employs an alternate approach. Following the network's training, a smoothing factor is applied. Every output unit establishes a dedicated connection with both a summation unit and a division unit. Notably, the normalization of the output vector is executed within the summation and output layers. The architecture employs linear transfer functions within the output layer, while the hidden layers operate with Radial Base functions. This nuanced approach sets GRNN apart from its predecessors, offering a distinctive structure and learning mechanism for data analysis and prediction tasks.

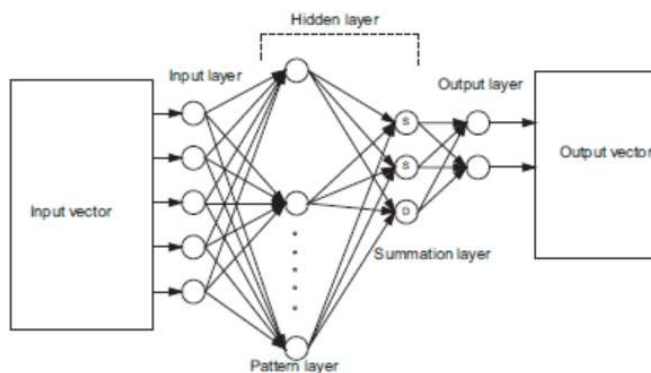


Figure 2.5: Generalized regression neural networks (image released as public domain [24])

4. **Adaptive neuro fuzzy systems:** Incorporating the reasoning capacity of fuzzy logic with the learning abilities of a neural network, ANFIS (Adaptive Neuro-Fuzzy Inference System) is a MLFFN variety that outperforms the capabilities of each approach when employed independently. There are Five layers of ANFIS structure that amplify prediction capabilities.

- i. **Fuzzy Layer:** Containing square nodes, the fuzzy layer is responsible for determining the membership strength of input data to a variety of linguistic terms. Represented by adjustable nodes, this initial layer is known for its fuzzy nature.
- ii. **Input Layer:** This layer is responsible for receiving the initial data input and transmitting it to the fuzzy layer. It assigns the input values to the membership functions depending on their respective degrees of membership.
- iii. **Consequent Layer:** is responsible for computing the ANFIS system's ultimate outcome. The nodes in this layer are illustrated as circles, and they integrate the fuzzy layer's outputs and their corresponding parameters.

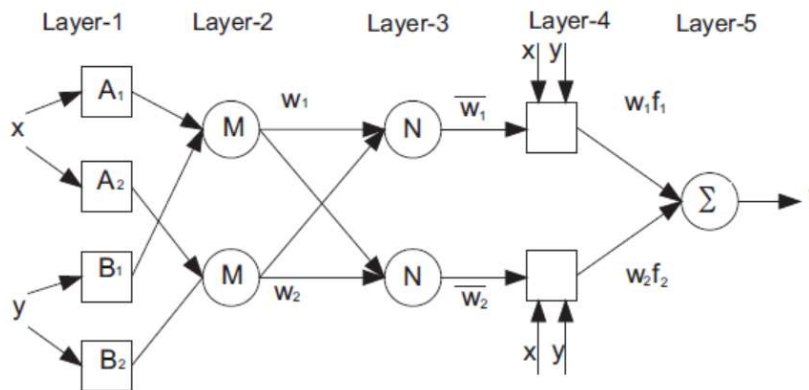


Figure 2.6: Adaptive neuro fuzzy systems (image released as public domain [25])

The contribution of each rule's output is adjusted by the Normalization Layer, which calculates the necessary normalization factors. Based on the combination of rule outputs from the previous layers, the ultimate output of the ANFIS system is generated by the final layer. Using back propagation techniques, ANFIS can alter its parameters while learning. ANFIS combines neural networks' learning abilities with fuzzy logic's linguistic handling to produce excellent outcomes in intricate systems, forecasts, and data analysis tasks, effectively processing both quantitative and qualitative information to make informed choices.

2.4.1. Applications

In **Vapor Compression Systems** performance prediction and assessment of chillers, heat pumps, refrigeration systems, compressors, thermophysical properties of refrigerants.

In Vapor Absorption Systems: Performance of multi effect absorption chiller, Optimization of Absorption Chiller Parameters, Chiller Fault Diagnosis.

In **HVAC Components** control of Evaporators, Control of AHUs, Control of Fans, Performance of Cooling towers, Control and Performance of Chilled Water Pumps, Static and Transient response of Heat Exchangers.

In **HVAC design** Energy consumption of buildings, Cooling Load forecasting, Thickness of Insulation to be used in a building.

In **Advanced Heating and Cooling** performance of gas cooler in Carbon Dioxide Heat Pump, Heating and Cooling performance of vortex tube, temperature prediction inside refrigerators, performance analysis of indirect evaporative cooling systems

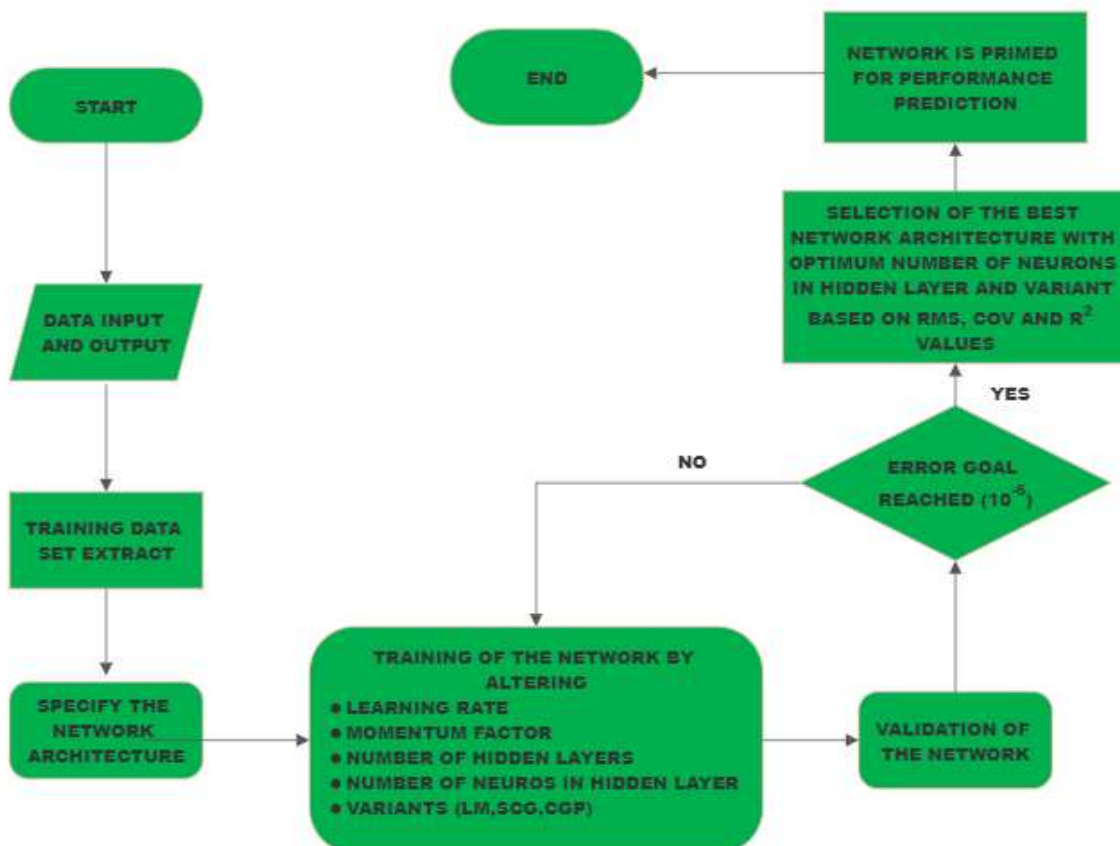


Figure 2.7: Process flowchart of Modelling ANN(Adapted from [22])

The above figure summarizes the entire process of modelling ANN for HVAC and generally for any other applications given.

The paper further goes on to identify the limitations of ANN namely:

- a.) **Overtraining:** Large number of training cycles required to reach precision target. As well as avoiding over fitting so as to not degrade prediction performance
- b.) **Extrapolation:** The range of the training data must represent the range of operating data so as to set the maximum and minimum values from experimental runs.
- c.) **Optimization:** Selection of optimum network parameters that actually influence the system.

Conclusively, Mohanraj, Jayaraj and Muraleedharan reviewed just over ninety published papers at their time of writing. There were several applications of ANN as were discussed above which not only showed their use cases but also exhibited their efficacy and reliability. The limitation and future works were also discussed in the field of RACHP.

Lukas et al applied ANN to predict the Absorption Chillers performance which utilized Solar energy as the heating source. Approaches of ANN were utilized from previous works on the topic but Back propagation MLFFN model was used to predict the performance (outlet temperature of cooling, hot and chilled water temperatures). Data for the ANN network was used from four different locations with cooling capacities ranging from 880kW to 1750kW. The input parameters used were Chilled Water Return Temperature, Cooling Water Return Temperature, Ambient Temperatures and Hot Water Temperatures (Some use cases required Hot Water). The time delay and number of nodes were varied to predict the optimum values of the above stated values. The results showed good agreement with that of Real-world Data with R2 values of 95%.[29]

2.5. Machine Learning Algorithms employed for prediction of COP for Absorption Chillers:

Manohar et. al embarked on a groundbreaking research endeavor, potentially the first of its kind, focusing on the application of Artificial Neural Networks (ANN) to a Double Effect Absorption Chiller powered by steam, an unconventional heat source. The architecture was constructed upon a Multi-Layer Feedforward Neural Network (MLFFN) employing back propagation for training. The inputs encompassed key parameters: Chilled Water Inlet and

Outlet Temperatures, Cooling Water Inlet and Outlet Temperatures, and Steam Pressure. The specific chiller examined possessed a capacity of 805kW and operated as a Series flow unit.

The training dataset incorporated a year's worth of real-world operational data. To expedite learning, a "flat spot elimination" technique was introduced. This technique addressed the issue of stagnant weights by modifying the derivative of the sigmoid function. By adding a constant value of 0.1 to the derivative, a functional error signal that could be back propagated was maintained as the unit's output neared 1.0. The research further incorporated variable biases, which involved adding a constant value node of 1 to each layer (excluding the output layer). This dynamic adaptation aided the learning algorithm in fine-tuning biasing values.

Upon establishing a consistent learning rate, the researchers conducted iterations to identify the point where the minimum R2 values were achieved. With 10,000 iterations, and subsequently extending to 12,000 iterations, a 0.3% increase in R2 value was observed. The network architecture implemented in this study followed a 6-6-9-1 configuration, with four layers. The initial layer consisted of the input parameters along with a time node. Two hidden layers were employed, demonstrating optimal results without a significant increase in computational time compared to a single hidden layer. The output layer's role was to predict the Coefficient of Performance (COP) of the absorption chiller.

Upon completion of the training, testing, and prediction phases, the study showcased highly promising outcomes. The predicted results closely aligned with actual COP values, with an R2 value approaching an impressive 99.9753% and an error margin of approximately $\pm 1.2\%$. This underscores the accuracy and efficacy of the developed ANN model in predicting the performance of the steam-powered Double Effect Absorption Chiller. [18]

Jee et. Al used ANN to forecast the energy consumption of an Absorption Chiller and Air Handling Unit of a particular facility and an. The inputs used for prediction of energy consumption of the Absorption Chiller were Cooling Water Supply and Inlet Temperature Ambient Air Conditions, Dry Bulb (DB) Temperature and Relative Humidity (RH). The Chiller Capacity was approximately 2100kW. The ANN architecture was 5-5-1 with just one hidden layer. However, despite proper modelling of the system the ANN was not able to predict Energy Consumption with high accuracy due to inconsistencies in the normalization of input data as well the data itself not being representative of the system to a high degree. The CV (RMSE) values reached approximately 30% which was undesirable owing to the reasons

mentioned. Also, the error rate reached a maximum of 15.18% due to high variance-low bias issue. [30]

Another study conducted by Jee et. Al considered predicting the Absorption Heat Pumps Energy consumption with 12 multilayer shallow neural network (MLNN) training algorithms. The results of the algorithms were compared and evaluated with that of real-world data for a month. All the algorithms were based on back propagation. The ANN architecture consisted of 20 neurons and 3 hidden layers. The input parameters used were Historical Energy Use, Seasonality Data, Dry Bulb Temperature and Relative Humidity as Ambient Condition Data and Finally Cooling water Supply rate and Temperature as operating condition.

Table 2: Max and Min Standard Deviation

Neural Network Algorithms	Error Rate			CvRMSE		
	Minimum (%)	Maximum (%)	Standard Deviation (SD)	Minimum (%)	Maximum (%)	Standard Deviation (SD)
BR	0.41	5.05	1.68	21.98	30.00	2.33
RP	0.59	13.59	4.91	24.31	28.12	1.27
SCG	0.04	15.16	5.07	24.29	29.30	1.45
CGB	0.07	10.14	2.99	24.33	29.49	1.49
CGP	0.13	5.73	1.76	24.89	29.97	1.48
BFG	0.95	9.78	2.82	23.13	27.92	1.75
LM	0.09	5.76	1.94	22.04	28.88	2.17
BR	0.41	5.05	1.68	21.98	30.00	2.33
CGF	0.58	15.58	4.81	21.08	30.69	3.13

GDX	0.92	17.40	5.75	26.16	37.11	3.66
OSS	0.03	26.07	8.16	24.76	38.05	4.13
GDM	0.30	41.77	14.82	32.25	53.20	7.11
GD	3.89	27.52	6.98	33.20	58.85	9.08

The above table summarizes the results and the success rate of the 12 algorithms employed in predicting the Absorption Heat Pumps' energy consumption. The most successful and typically utilized models for nonlinear regression predictions which were the LM (Levenberg-Marquardt) and BR (Bayesian Regularization) achieved agreeable results if not the most accurate results.[34]

Panahizadeh et al. Used multilayer perceptron ANN with error backpropagation algorithm in conjunction with hyperbolic tangent as the excitation function and Levenberg-Marquardt Learning Method with 15285 data points. The inputs for the ANN were cooling water inlet temperature, chilled water inlet temperature, inlet steam temperature, outlet chilled water temperature and Solution Heat Exchanger Efficiency Respectively. The outputs of the ANN were COP and the thermal energy input required. The Capacity of the Single Effect Absorption Chiller was 4775 kW. The network architecture was 2-10-5 with a single hidden layer. The prediction was successful as the results were highly accurate as the mean square error came out to be approximately 3.2×10^{-7} for COP and 7.5×10^{-8} for Thermal energy consumption.[37]

Chapter 3. System Description

3.1. System Description

The system proposed for this research study is that of a Direct Fired Parallel Flow Absorption Chiller. The main reason for the selection of such a system was that it is the most commercially available system with the highest COP. Advanced multi effect systems especially Triple Effect Absorption Refrigeration Systems and Cascade refrigeration systems that use both compressors and heat generators have also been studied and are under further study. These systems have shown both increased COP and much greater Exergetic efficiency. Furthermore, they have exhibited greater part load performances. However, the above-mentioned systems are much too complex to operate and maintain. Not to mention the high investment cost associated with them at this point in time. Conversely, the decision to focus this study on Double effect parallel flow systems was also that the real world data, that was needed, was also relatively easily available with which validation of both the Energy and Exergy Model and Machine Learning Model could be done.

Firstly, we shall delve into the system specifics and working principle The Double Effect Absorption Chiller System which from this point forward shall be referred to as DEAC system. Then we shall conduct First (Energy) and Second (Exergy) law Analysis of the DEAC System. Many studies have previously been done on the Energy and Exergy Analysis of the DEAC System both in series flow and parallel flow and other novel configurations or combinations as discussed in CHAPTER-2. This shall form the basic framework for the EES model from which we shall determine the theoretical COP of the DEAC System.

3.2. Working Principle:

The DEAC system is an advancement of the Single Effect Absorption Chiller System which can utilize energy from higher grade heat sources more efficiently.

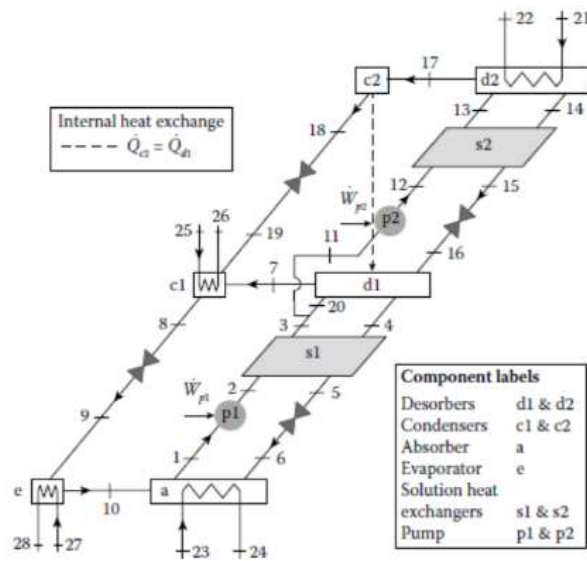


Figure 3.1: Duhring Plot Parallel flow DEAC (Adapted from [29])

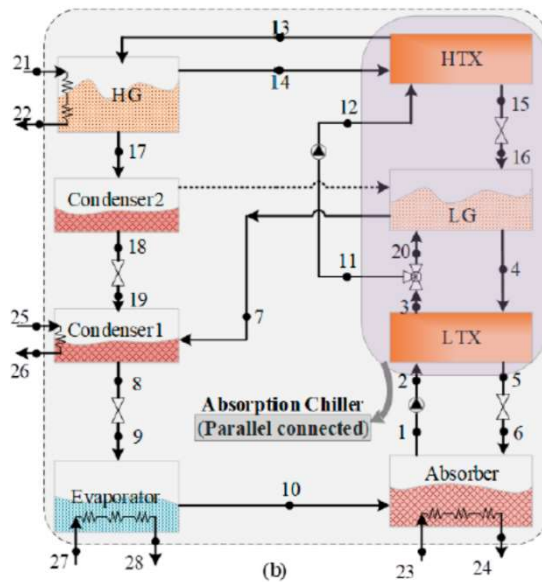


Figure 3.2: Schematic of Parallel Flow DEAC (Adapted from [30])

In Figure 3.2, a schematic representation of a parallel flow Double Effect Absorption Chiller (DEAC) is shown, while Figure 3.1 displays the Duhring Plot depicting the same cycle. The DEAC system utilizes two Solution Heat Exchangers, designated for the High and Low Temperature Desorbers/Regenerators. Operating at three pressures and three temperatures, the DEAC system's operational stages are as follows:

1. The strong LiBr-H₂O solution exits the absorber (state 1) and enters the pump as a saturated liquid.

2. The high-pressure saturated liquid from the pump enters the Low Temperature Solution Heat Exchanger (LTX) for preheating by interacting with the returning weak solution from state 4.
3. After leaving the LTX, the preheated solution splits into two streams. The first stream (state 11) goes to the High Temperature Solution Heat Exchanger (HTX) at state 12. Similarly, this solution undergoes further preheating by interacting with the returning weak solution from state 13 within the HTX.

Within the High Temperature Generator, the preheated strong solution stream of the LiBr-H₂O refrigerant pair undergoes boiling, fueled by an external heat source – in this case, a Natural Gas Fired Burner. This process results in complete separation of the mixture, with the exiting stream typified as pure water at state 17. The refrigerant stream is then condensed in condenser 2, utilizing its heat for the Low Temperature Generator to form a saturated vapor at state 7. The vapor-liquid mixture from state 17 passes through an expansion valve, reducing its pressure to the level of the Low Generator (LG), resulting in a vapor-liquid mixture at state 19. Both the solution streams from state 7 and state 19 release heat to the cooling water in condenser 1. The refrigerant's temperature is equilibrated with that of the absorber by passing through another expansion valve. This cooled stream extracts heat from the returning chilled water stream sourced from HVAC or Process Returned Water.

The less concentrated solution of aqueous LiBr originating from state 15 undergoes a decrease in pressure via an expansion valve to attain the same pressure level as the Low Generator (LG), denoted as state 16. During this process, heat is released to the stronger solution, leading to its transformation into state 4. This further-diluted solution subsequently proceeds through the Low Temperature Solution Heat Exchanger (LTX), releasing heat to the stronger solution. Ultimately, after relinquishing the remaining heat to the incoming concentrated solution, the weaker solution reaches state 5. A subsequent passage through another expansion valve brings it to state 6, marking its entry into the absorber. In the absorber, it mingles with the vapor stream from state 10 and the concentrated solution already present. The heat is released from the absorber and transferred to the cooling water stream as part of the cooling process.

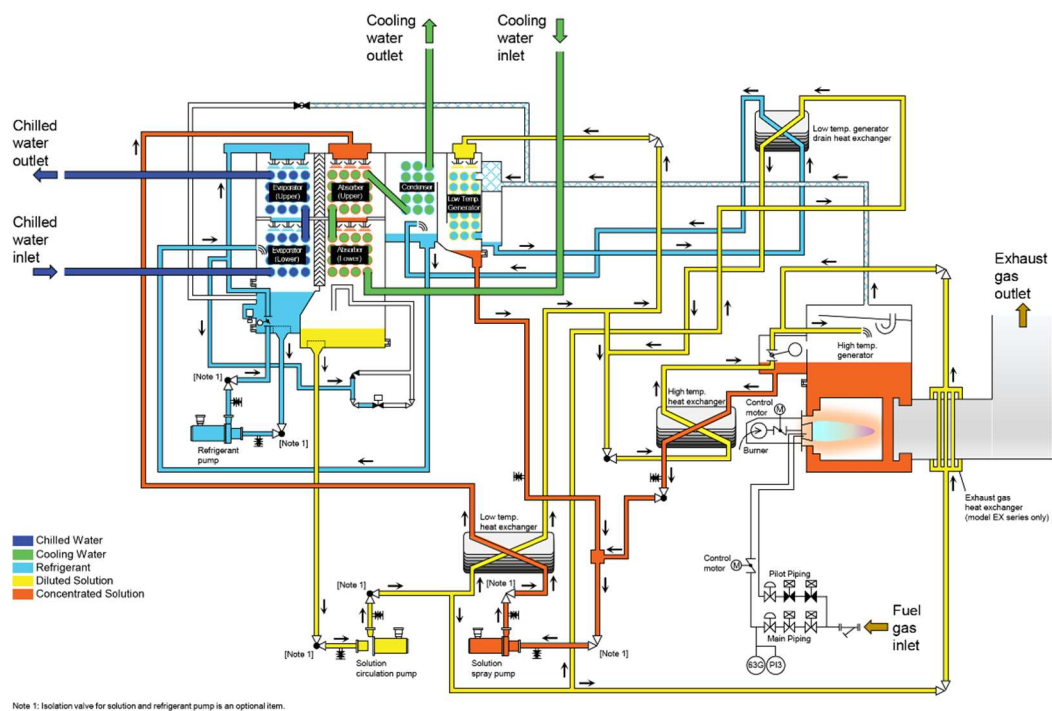
3.3. Specifications of the Proposed System

The Table below outlines the key specifications of the actual DEAC System upon which this study is based. The effective USTR is 500 for DEAC system of the particular system under study even though its actual capacity is 560 USTR.

However, over the course of time, fouling in the heat exchangers, reduced pump efficiency and lack thereof proper maintenance has had an adverse effect on capacity.

Table 3: Key specifications of the actual DEAC System

Model	WCDN056SK61
Cooling-Capacity	560 USTR/1969 kW (Effectively 500 USTR)
Chilled-Water-Flow Rate	1333 USGPM
Cooling-Water-Flow Rate	2465 USGPM
Fuel Consumption Rate	161.7 Nm ³ /h
Electrical Consumption Data	14.9 kW



LD31222

Figure 3.3: OEM Process flow of the Proposed DEAC System (available to public domain [42])

The above figure shows the actual system schematic of the proposed system under study. The main thing to observe is that in a Direct Fired DEAC system, the high temperature generator is basically a fire tube heat exchanger. The strong solution mixture is passed through the tubes which are exposed to the Combustion Chamber. This heats the solution and separates the refrigerant mixture.

3.3.1. Purge System

The purge system in an absorption chiller refers to a subsystem or mechanism that helps remove non-condensable gases (NCGs) from the chiller's refrigerant-absorbent solution. Non-condensable gases are gases that cannot be easily condensed into liquid form and can accumulate within the chiller system over time. The presence of these gases can negatively impact the chiller's efficiency and performance, leading to reduced cooling capacity and increased energy consumption. The purge system is designed to address this issue and maintain the optimal functioning of the absorption chiller.[45]

The key components and functioning of a purge system in an absorption chiller are as follows:

1. **Purge Unit:** The purge unit is a dedicated component or subsystem within the absorption chiller that is responsible for removing non-condensable gases. It is usually located at a strategic point within the chiller system, often in the generator or another high-temperature part of the cycle.
2. **Purge Valve:** A purge valve is integrated into the purge unit. This valve is opened periodically to release a controlled amount of refrigerant-absorbent solution along with the accumulated non-condensable gases. The released mixture is sent to the atmosphere or a designated disposal system.
3. **Purge Timing:** The timing of purging is crucial. The purge valve is typically operated during periods when the chiller system is not in active cooling mode. This ensures that purging does not interfere with
4. **Purge Control:** Purging is controlled by the chiller's control system. Sensors and detectors are used to monitor the concentration of non-condensable gases within the refrigerant-absorbent solution. When the concentration exceeds a certain threshold, the control system triggers the purge valve to open.

5. Purge Efficiency: The efficiency of the purge system is important. Effective purging ensures that the concentration of non-condensable gases remains at an acceptable level, minimizing their impact on the chiller's operation.

3.3.2. Benefits of Purging:

The removal of non-condensable gases through purging helps maintain the chiller's heat transfer efficiency by preventing the build-up of insulating gases. This, in turn, enhances the chiller's performance, improves its coefficient of performance (COP), and reduces energy consumption.

3.4. Crystallization

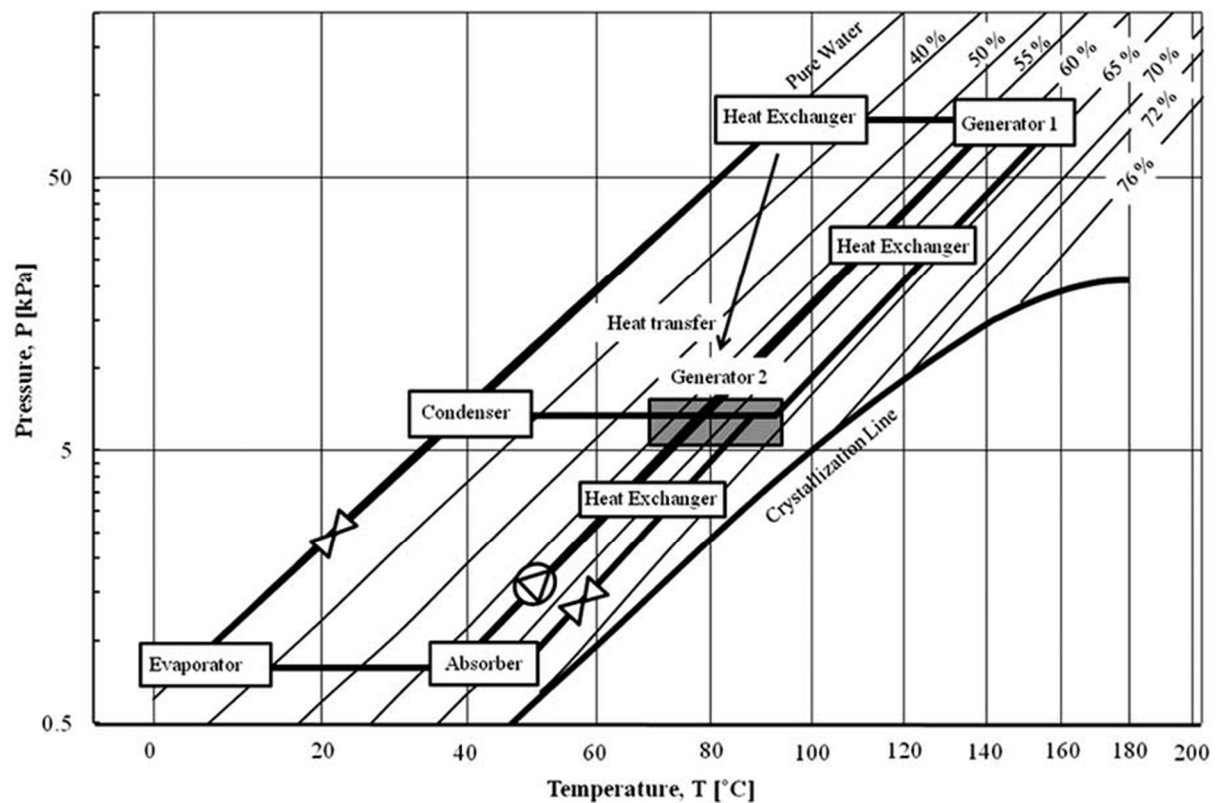


Figure 3.4: Temperature Vs Pressure Plot Indicating DEAC Parallel flow Thermodynamics above Crystallization line (adapted from [27])

The illustration in Figure 3.4 clearly shows that the parallel flow configuration's operating conditions are considerably more distant from the crystallization line of the LiBr-H₂O solution in comparison to the series flow arrangement. Moreover, owing to the significantly diminished solution flow rate directed towards the high temperature generator, there is a substantial

decrease in both the generator's internal pressure and its elevation. Crystallization in an absorption chiller refers to the formation of solid crystals within the chiller's refrigerant-absorbent solution. This phenomenon occurs when certain components of the solution, such as the absorbent material (e.g., lithium bromide), start to crystallize due to changes in temperature, concentration, or other operating conditions. Crystallization can have detrimental effects on the chiller's performance, efficiency, and overall operation.

3.4.1.1. Adverse effects of Crystallization on the Absorption Cycle:

1. **Reduced Heat Transfer:** Crystals that form within the solution can hinder the flow of the liquid and disrupt heat transfer processes. This can lead to decreased efficiency in heat exchange within the chiller's components, such as the evaporator, absorber, and generator.
2. **Flow Restrictions:** Crystals can accumulate and create blockages or restrictions in the flow paths of the solution. This can result in reduced flow rates, increased pressure drop, and uneven distribution of the solution, affecting the chiller's overall performance.
3. **Reduced Cooling Capacity:** Crystallization can lead to a decrease in the amount of absorbent available in its liquid form. This reduction in the effective concentration of the absorbent can result in a lower capacity to absorb refrigerant vapor, leading to reduced cooling capacity and lower coefficient of performance (COP).
4. **Corrosion and Erosion:** Crystals can contribute to the erosion of surfaces within the chiller's components. As crystals flow through the system, they can cause abrasion and wear on surfaces, potentially leading to corrosion and damage over time.
5. **System Shutdown:** Severe crystallization can lead to the chiller's shutdown or even damage to its components. For instance, if crystals accumulate in the heat exchangers or other critical parts, they can interfere with proper heat exchange, causing overheating and potential system failure.
6. **Maintenance and Cleaning:** To mitigate the effects of crystallization, maintenance procedures may be required to clean out or remove crystals from the chiller's components. This can result in downtime and increased maintenance costs.

Preventing or managing crystallization in an absorption chiller involves careful design, operation, and maintenance strategies. These can include:

Operating Conditions: Maintaining stable operating conditions, such as temperature and pressure, can help prevent or minimize crystallization. Adequate insulation of components can also prevent temperature fluctuations.

Absorbent Concentration: Keeping the concentration of the absorbent within a suitable range can prevent crystallization. Dilution or replenishment of the solution may be necessary in some cases.

Anti-Crystallization Additives: Some absorption chiller systems may use additives or chemicals to inhibit or control crystallization within the solution.

Regular Maintenance: Regular inspection and maintenance of the chiller's components can help detect and address crystallization issues before they become severe.[45]

3.5. Thermodynamic Analysis of the DEAC System:

3.5.1. General Equations:

Mass-Balance:

$$\sum \dot{m}_{in} = \sum \dot{m}_{out} \quad (1)$$

Where \dot{m}_{in} and \dot{m}_{out} represent mass flow rate of a pure substance entering and exiting a control volume.

Mixture-Balance:

$$\sum \dot{m}_{in}X_{in} = \sum \dot{m}_{out}X_{out} \quad (2)$$

Where $\dot{m}_{in}X_{in}$ and $\dot{m}_{out}X_{out}$ represent mass flow rate of a mixture entering and exiting a control volume.

Energy-Conservation:

$$\sum \dot{Q} - \sum \dot{W} = \sum \dot{m}_{out} h_{out} - \sum \dot{m}_{in} h_{in} \quad (3)$$

The energy balance equation for the components of the system ignoring effects of Kinetic and Potential Energy due to steady state conditions. Where:

Where \dot{Q} represents the sum of all Heat rates entering or exiting the system.

Where \dot{W} represents the sum of all Work rates entering or exiting the system.

Where \dot{m} represents the sum of all mass flow rates entering or exiting the system.

Where h represents the sum of all enthalpies entering or exiting the system.

3.5.2. Heat-Transfer-Equation:

$$\dot{Q} = UA\Delta T_{LMTD} \quad (3.1)$$

$$\Delta T_{LMTD} = \frac{(T_{H,in} - T_{C,out}) - (T_{H,out} - T_{C,in})}{\ln(T_{H,in} - T_{C,out}) / (T_{H,out} - T_{C,in})} \quad (4)$$

The heat transfer eqn used to determine the heat exchanged between two fluids.

Where \dot{Q} represents the Heat rate entering or exiting the system.

Where U represents the Heat Transfer Coefficient.

Where ΔT_{LMTD} represents the mean temperature difference.

Where A represents the Heat Transfer Surface Area.

Where $T_{H,in}$ represents the Inlet Temperature of Hot Fluid.

Where $T_{H,out}$ represents the Outlet Temperature of Hot Fluid.

Where $T_{C,in}$ represents the Inlet Temperature of Cold Fluid.

Where $T_{C,out}$ represents the Outlet Temperature of Cold Fluid.

Pump-Work:

$$\dot{W}_p = \frac{\dot{m} \cdot V \cdot (P_f - P_i)}{\eta_{Pump}} \quad (5)$$

Where \dot{W}_p represents the Pump work rate.

Where V represents the specific volume of the fluid being pumped.

Where η_{Pump} represents the efficiency in converting electrical work to mechanical energy.

P_f & P_i Represents the final and initial pressures of the working fluid.

Exergy-Destruction:

$$\dot{E}Di = \sum \dot{E}_{in} - \sum \dot{E}_{out} - \left[\sum \left(\dot{Q} \left(1 - \frac{T_0}{T} \right) \right)_{in} + \sum \left(\dot{Q} \left(1 - \frac{T_0}{T} \right) \right)_{out} \right] - \sum \dot{W} \quad (6)$$

$\dot{E}Di$ Represents the Rate of Exergy Destruction occurring in the process occurring in the component.

$\sum \dot{E}_{in} - \sum \dot{E}_{out}$ Represents the exergy of the fluid streams entering and exiting the control volume.

The third and fourth terms represent the sum of the exergy of streams associated with heat transfer from the source maintained at constant Temperature T and is equal to the work obtained by a Carnot engine operating between T & T_0 entering and leaving the control volume.

The final term is the mechanical work rate being done in the control volume.

Energy-Efficiency:

$$\dot{W}_p = \frac{\dot{m} \cdot V \cdot (P_f - P_i)}{\eta_{Pump}} \quad (5)$$

$$COP = \frac{\dot{Q}_e}{(\dot{Q}_g + \dot{W}_e)} \quad (6)$$

COP is the Coefficient of Performance is the the ratio of useful cooling to the sum of the energy input.

\dot{Q}_e is the cooling load at the evaporator.

\dot{Q}_g is the heat input in the High Temperature Generator.

\dot{W}_e is the work input of solution pumps and other electrical auxiliaries.

Exergetic-Efficiency:

$$\eta_{ex} = \frac{\dot{Q}_e \left| \left(1 - \frac{T_0}{T_e} \right) \right|}{\dot{Q}_g \left(1 - \frac{T_0}{T_g} \right) + \dot{W}_e} \quad (7)$$

η_{ex} is the exergetic efficiency of the systems which exhibits the effectiveness of a system relative to its performance in reversible conditions.

\dot{Q}_e is the cooling load at the evaporator.

\dot{Q}_g is the heat input in the High Temperature Generator.

\dot{W}_e is the work input of solution pumps and other electrical auxiliaries.

T_0 is the initial ambient temperature.

T_e is the evaporator temperature.

T_g is the High temperature Generator.

Cost of Cooling using Exergo-economic analysis:

$$\dot{C}_{cool} = 1144.3 (\dot{Q}_{cool}) + 3\%(1144.3 (\dot{Q}_{cool})) \quad (8)$$

Where \dot{Q}_{cool} is the cooling load at the evaporator.

3.5.3. Equations for Heat Exchangers:

Absorber:

$$\dot{Q}_a = UA_a \frac{(T_{strong,abs} - T_{Cool,out}) - (T_{weak,abs} - T_{Cool,in})}{\ln\left(\frac{T_{strong,abs} - T_{Cool,out}}{T_{weak,abs} - T_{Cool,in}}\right)} \quad (9)$$

Condenser-1:

$$\dot{Q}_{CD,1} = UA_{CD,1} \frac{(T_{CWR} - T_{Cool,out}) - (T_{CWS} - T_{Cool,in})}{\ln\left(\frac{T_{CWR} - T_{Cool,out}}{T_{CWS} - T_{Cool,in}}\right)} \quad (10)$$

Evaporator:

$$\dot{Q}_e = UA_e \frac{(T_{CHWR} - T_{vapor,evap}) - (T_{CWS} - T_{Cool,in})}{\ln\left(\frac{T_{CHWR} - T_{Cool,out}}{T_{CWS} - T_{Cool,in}}\right)} \quad (11)$$

Heat Rate of Burner:

$$\dot{Q}_{HG} = \frac{\text{Gas Consumption Rate}}{\text{Gross Calorific Value of Fuel}} \times \eta_{\text{Burner}} \quad (12)$$

3.6. Component wise break down of mass balance, energy balance and Exergy Destruction:

Table 4: Component wise break down of mass balance, energy balance and Exergy Destruction:

System Components	Mass Balance	Energy Balance	Exergy Destruction
Absorber	$\dot{m}_1 x_1 = \dot{m}_6 x_6 + \dot{m}_{10} x_{10}$	$\dot{Q}_a = \dot{m}_6 h_6 + \dot{m}_{10} h_{10} - \dot{m}_1 h_1$	$\dot{E}x_{dest,a} = \dot{m}_6 ex_6 + \dot{m}_{10} ex_{10} - \dot{E}x_{th,a} - \dot{m}_1 ex_1$ $\dot{E}x_{th,a} = \left(1 - \frac{T_0}{T_a}\right) \dot{Q}_a$ $ex_1 = (h_1 - h_0) - T_0(s_1 - s_0)$ $ex_6 = (h_6 - h_0) - T_0(s_6 - s_0)$ $ex_{10} = (h_{10} - h_0) - T_0(s_{10} - s_0)$
Solution Pump-1	$\dot{m}_1 = \dot{m}_2$	$\dot{W}_{p1} = \frac{\dot{m}_1 \cdot V_1 \cdot (P_2 - P_1)}{\eta_{\text{Pump}}}$ $\dot{W}_{p1} = \dot{m}_2 h_2 - \dot{m}_1 h_1$	$\dot{E}x_{dest,p} = \dot{m}_1 ex_1 + \dot{W}_{p1} - \dot{m}_2 ex_2$ $ex_1 = (h_1 - h_0) - T_0(s_1 - s_0)$

			$ex_2 = (h_2 - h_0) - T_0(s_2 - s_0)$
LTX (Low Temperature Heat Exchanger)	$\dot{m}_2 + \dot{m}_4 = \dot{m}_3 + \dot{m}_5$	$\dot{m}_2 h_2 + \dot{m}_4 h_4$ $= \dot{m}_3 h_3 + \dot{m}_5 h_5$	$ex_2 = (h_2 - h_0) - T_0(s_2 - s_0)$ $ex_4 = (h_4 - h_0) - T_0(s_4 - s_0)$ $ex_3 = (h_3 - h_0) - T_0(s_3 - s_0)$ $ex_5 = (h_5 - h_0) - T_0(s_5 - s_0)$ $\dot{E}x_{dest,LTX} = \dot{m}_2 ex_2 + \dot{m}_4 ex_4 - \dot{m}_3 ex_3 - \dot{m}_5 ex_5$
LG (Low Pressure Generator)	$\dot{m}_{20} + \dot{m}_{16} = \dot{m}_7 + \dot{m}_4$	$\dot{Q}_{LG} = \dot{Q}_{CD2}$ $\dot{Q}_{LG} = \dot{m}_{20} h_{20} + \dot{m}_{16} h_{16} - \dot{m}_7 h_7 - \dot{m}_4 h_4$	$\dot{E}x_{dest,LG} = \dot{m}_7 ex_7 + \dot{m}_4 ex_4 - \dot{m}_{20} ex_{20} - \dot{m}_{16} ex_{16} - \dot{E}x_{th,LG}$ $\dot{E}x_{th,LG} = \left(1 - \frac{T_0}{T_{LG}}\right) \dot{Q}_{LG}$ $ex_4 = (h_4 - h_0) - T_0(s_4 - s_0)$ $ex_7 = (h_7 - h_0) - T_0(s_7 - s_0)$ $ex_{16} = (h_{16} - h_0) - T_0(s_{16} - s_0)$ $ex_{20} = (h_{20} - h_0) - T_0(s_{20} - s_0)$

Solution Pump-2	$\dot{m}_{11} = \dot{m}_{12}$	$\dot{W}_{p2} = \frac{\dot{m}_{11} \cdot V_{11} \cdot (P_{12} - P_{11})}{\eta_{Pump}}$ $\dot{W}_{p2} = \dot{m}_{12} h_{12} - \dot{m}_{11} h_{11}$	$\dot{E}x_{dest,p2} = \dot{m}_{11} ex_{11} + \dot{W}_{p1} - \dot{m}_{12} ex_{12}$ $ex_{11} = (h_{11} - h_0) - T_0(s_{11} - s_0)$ $ex_{12} = (h_{12} - h_0) - T_0(s_{12} - s_0)$
HTX (High Temperature Heat Exchanger)	$\dot{m}_{12} + \dot{m}_{14} = \dot{m}_{13} + \dot{m}_{15}$	$\dot{m}_{12} h_{12} + \dot{m}_{14} h_{14} = \dot{m}_{13} h_{13} + \dot{m}_{15} h_{15}$	$ex_{12} = (h_{12} - h_0) - T_0(s_{12} - s_0)$ $ex_{14} = (h_{14} - h_0) - T_0(s_{14} - s_0)$ $ex_{13} = (h_{13} - h_0) - T_0(s_{13} - s_0)$ $ex_{15} = (h_{15} - h_0) - T_0(s_{15} - s_0)$ $\dot{E}x_{dest,LTX} = \dot{m}_{12} ex_{12} + \dot{m}_{14} ex_{14} - \dot{m}_{13} ex_{13} - \dot{m}_{15} ex_{15}$
HG (High Pressure Generator)	$\dot{m}_{13} = \dot{m}_{14} + \dot{m}_{17}$	$\dot{Q}_{HG} = \dot{m}_{14} h_{14} + \dot{m}_{17} h_{17} - \dot{m}_{13} h_{13}$	$\dot{E}x_{dest,LG} = \dot{m}_{13} ex_{13} + \dot{E}x_{th,LG} - \dot{m}_{17} ex_{17} - \dot{m}_{14} ex_{14}$ $\dot{E}x_{th,HG} = \left(1 - \frac{T_0}{T_{HG}}\right) \dot{Q}_{HG}$ $ex_{13} = (h_{13} - h_0) - T_0(s_{13} - s_0)$ $ex_{14} = (h_{14} - h_0) - T_0(s_{14} - s_0)$

			$ex_{17} = (h_{17} - h_0) - T_0(s_{17} - s_0)$
Condenser-2	$\dot{m}_{17} = \dot{m}_{18}$	$\dot{Q}_{CD2} = \dot{Q}_{LG}$ $\dot{Q}_{CD2} = \dot{m}_{18}h_{18} - \dot{m}_{17}h_{17}$	$\dot{E}x_{dest,CD2} = \dot{m}_{17}ex_{17} + \dot{E}x_{th,LG} - \dot{m}_{18}h_{18}$ $ex_{17} = (h_{17} - h_0) - T_0(s_{17} - s_0)$ $ex_{18} = (h_{18} - h_0) - T_0(s_{18} - s_0)$
Condenser-1	$\dot{m}_{19} = \dot{m}_8$	$\dot{Q}_{CD} = \dot{m}_8h_8 - \dot{m}_{19}h_{19}$	$\dot{E}x_{dest,CD1} = \dot{m}_8ex_8 + \dot{E}x_{th,CD1} - \dot{m}_{19}h_{19}$ $ex_8 = (h_8 - h_0) - T_0(s_8 - s_0)$ $ex_{19} = (h_{19} - h_0) - T_0(s_{19} - s_0)$
Evaporator	$\dot{m}_9 = \dot{m}_{10}$	$\dot{Q}_E = \dot{m}_{10}h_{10} - \dot{m}_9h_9$	$\dot{E}x_{dest,E} = \dot{m}_9ex_9 + \dot{E}x_{th,E} - \dot{m}_{10}ex_{10}$ $\dot{E}x_{th,E} = \left(1 - \frac{T_0}{T_E}\right)\dot{Q}_E$ $ex_9 = (h_9 - h_0) - T_0(s_9 - s_0)$ $ex_{10} = (h_{10} - h_0) - T_0(s_{10} - s_0)$
Solution Valve-1	Expansion $\dot{m}_5 = \dot{m}_6$	$\dot{m}_5h_5 = \dot{m}_6h_6$	$\dot{E}x_{dest,SEV,1} = \dot{m}_5ex_5 - \dot{m}_6ex_6$

Solution Valve-2	Expansion	$\dot{m}_{15} = \dot{m}_{16}$	$\dot{m}_{15}h_{15} = \dot{m}_{16}h_{16}$	$\dot{E}x_{dest,SEV,2} = \dot{m}_{15}ex_{15} - \dot{m}_{16}ex_{16}$
Refrigerant Valve-1	Expansion	$\dot{m}_{18} = \dot{m}_{19}$	$\dot{m}_{18}h_{18} = \dot{m}_{19}h_{19}$	$\dot{E}x_{dest,REV,1} = \dot{m}_{18}ex_{18} - \dot{m}_{19}ex_{19}$
Refrigerant Valve-2	Expansion	$\dot{m}_8 = \dot{m}_9$	$\dot{m}_8h_8 = \dot{m}_9h_9$	$\dot{E}x_{dest,REV,2} = \dot{m}_8ex_8 - \dot{m}_9ex_9$

The above table forms the basis of this studies' Thermodynamic EES from which theoretical COP shall be calculated.

Table 5: Theoretical COP Calculation Parameters.

State Points	State	Remarks
1	Saturated Liquid Mixture	Assumed Vapor Quality set to 0
2	Subcooled Liquid Mixture	Determined from Pump model
3	Subcooled Liquid Mixture	Determined from LTX model
4	Saturated Liquid Mixture	Assumed Vapor Quality set to 0
5	Subcooled Liquid Mixture	Determined from LTX model
6	Liquid, Vapor Mixture	Quality of Vapor Determined from SEV-1 Model
7	Superheated Water Vapor	Assumed to be pure water

8	Saturated Liquid Water	Assumed Vapor Quality set to 0
9	Vapor, Liquid water state	Quality of Vapor Determined from REV-1 Model
10	Saturated Water Vapor	Assumed Vapor Quality set to 1
11	Saturated Liquid Mixture	Assumed Vapor Quality set to 0
12	Subcooled Liquid Mixture	Determined from Pump model
13	Subcooled Liquid Mixture	Determined from HTX model
14	Saturated Liquid Mixture	Assumed Vapor Quality set to 0
15	Subcooled Liquid Mixture	Determined from HTX model
16	Liquid, Vapor Mixture	Quality of Vapor Determined from SEV-2 Model
17	Superheated Water Vapor	Assumed to be pure water
18	Saturated Liquid water	Assumed Vapor Quality set to 0
19	Vapor, Liquid water state	Quality of Vapor Determined from REV-2 Model
20	Subcooled Liquid Mixture	Determined from LTX model

Chapter 4. Overview of Machine Learning Methods

It has already been discussed in CHAPTER 2 at length, of the applications and merits of using Machine Learning and Artificial Neural Networks (ANN) in the HVAC domain. However, the main focus of this CHAPTER is to deliver an indication of the Algorithms used in ANN. Additionally, the proposed Machine Learning model used for determining the COP of the DEAC system used in this study, will be discussed detail regarding the process of developing this proposed network architecture.

4.1. Overview of Machine Learning Models & ANN Algorithms:



Figure 4.1: Machine Learning (Adapted from [37])

Machine Learning is a subset of AI (Artificial Intelligence) which focuses on the development of advanced algorithms that enable computers to learn intelligently and make accurate predictions. The key objective is the correlation of non-linear relationships saves time without the need of advanced empirical formulations and deep domain knowledge [39, 41]. The above Figure 4.1 depicts the three major areas of classification and their subcategories as explained below:

Supervised Learning: The model is proficient on a labelled dataset. The input and corresponding output data are fed into the model. The model will learn to correlate output data with the provided input data by virtues of altering weights and biases and error correction and optimization techniques. The trained model fixes the weights when the agreeable accuracy is achieved. Then the model will make predictions on new input data [42, 48].

There are two sub-classifications of supervised learning [51]:

- **Classification:** This pertains to sorting of input data into present classification parameters known as categorical labels. For example predicting whether a student will Pass or Fail based on his past academic performance. Typically used algorithms for classification are Naïve-Bayes, Support Vector Machines, and Logistic Regression etc.
- **.Regression:** This pertains to predicting as certain continuous numerical value such as predicting the COP of a DEAC System based on the given input parameters. Typically used algorithms for regression are Ensemble Methods, Linear Regression, and Decision Trees etc.

Unsupervised Learning: Unlike supervised learning, in this approach, unlabelled data is fed to the model that must find correlational patterns on its own. Dimensionality reduction and Clustering are common tasks used for unsupervised learning.

Dimensionality Reduction: Technique used in machine learning to reduce the number of features i.e. inputs in a dataset. Too many dimensions can increase noise in the output signal, increase processing time or increase redundancy which was not required.

There are 2 broader subcategories:

Feature Selection: This involves selecting the most informative and influential features of a subset and eliminate unnecessary dimensions. The three methods used for this are Filter methods, Wrapper Methods and Embedded Methods.

Feature Extraction: It creates new features derived from the provided feature subset to reduce dimensions by combining or transformation of the original input signals. It uses techniques like Principle Component Analysis (PCA), Linear Discriminant Analysis (LDA), t-Distributed Stochastic Neighbour embedding (t-SNE) and Auto encoders.

Clustering: It is the assignment of a set of objects with similar characteristics (clusters) into subsets. There are 5 key concepts:

Data Points: Samples of the input dataset.

Features: Dimensions that describes the data point.

Distance Metric: A metric used to quantify the similarity or lack thereof between data points. Euclidean Distance, Cosine Similarity and Manhattan Distance are typical metrics used.

Cluster: The actual clustering based on previous three concepts and similarities of data points.

Centroid: The mean of the features or dimensional values of the data points in a cluster.

The popular algorithms used for clustering are **K-Means, Hierarchical, DBSCAN, Mean Shift, Gaussian Mixture Modelling, Spectral, Agglomerative** etc.[13,48]

Reinforcement Learning: As the name suggests, it is a reward based learning model. It involves an agent interacting with the environment and being presented with different scenarios. The agent makes a series of decisions to achieve a long term objective by being rewarded for every correct decision. The following are the key components of Reinforcement Learning.

- **Agent:** The entity which performs the action to gain rewards.
- **Environment:** The Scenario faced by the Agent.
- **State:** The situation of the Environment.
- **Action:** Choice made by the agent for interaction with the environment. Dependent on the policy
- **Policy:** Strategy applied by the agent to decide next action based on current state being faced to maximize cumulative award.
- **Reward:** Numerical value received by the agent either positive or negative as an outcome of the decision taken by the agent. The agents' goal is to maximize cumulative rewards over time.
- **Value Function:** A function that estimates the expected cumulative reward an agent can achieve from a given state according to specific policy. It assists the agent in

evaluating the desirability of the various states. Some of the key concepts of Reinforcement learning are Exploration vs Exploitation, Markov Decision Process (MDP), Policy Optimization, Value Based Methods, Policy Based Methods and Model-Based Vs. Model Free methods.[42,47]

4.1.1. Artificial Neural Networks:

Artificial Neural Networks are computational algorithms which mimic the structure and function of Neurons in a human brain. It is the fundamental building block of both Machine Learning and Deep Learning.

Figure below shows structure of a conceptual ANN with the key components further discussed below.

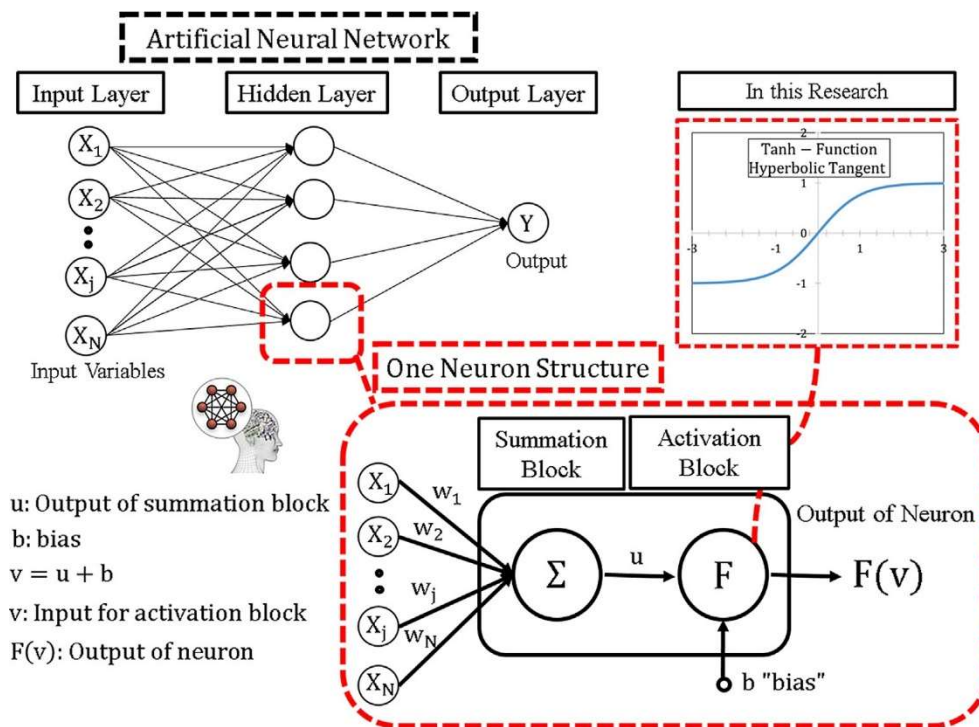


Figure 4.2: Structure of a Neuron(available to public domain [46])

4.1.2. Components of ANN:

1. **Node (Neuron):** This is the essential foundational block that forms the basis of ANN. Each and every neuron takes an input dataset, performs complex mathematical computations and returns an output.

2. **Weights and Biases:** These represent the strength of the interlinkages between nodes. Each neuron has a bias that shifts the output to the desired state.
3. **Activation Function:** The main objective of ANNs' is to correlate nonlinear relationships and produce a desired result. However, an activation function reduces the non-linearity to enable ANNs' to determine and achieve desired results.
4. **Layers:** There are three layers in an ANN:
5. **Input:** This layer receives points to the raw input feature data and passes it along the subsequent layers.
6. **Hidden Layer:** This is the processing layer which performs complex arithmetic calculations and feature extraction while extrapolating and manipulating the input data from the input layer.
7. **Output Layer:** This layer is responsible for producing an output of the computational results received from the hidden layer or layers.

There are several key processes that take place between the layers and within the layers themselves to bring about the desired results. Outlined below is a brief description of these processes:

1. **Forward Propagation:** The input data is passed along through the network layer by layer, computations at each node produces an output which forms the prediction.
2. **Loss Function:** This can be counted as a metric of the difference between the predicted output and the desired targeted results. The key objective here is to minimize this difference during training.
3. **Backpropagation:** This is the process through which weights and biases are adjusted for training of the ANN. In an order to reduce the error or difference percentage between actual and predicted results, weights and biases are sensitively adjusted in every pass through of the dataset through the neural network. This enhances the reliability and accuracy of the prediction model.
4. **Optimization:** Mathematical techniques optimize the loss function iteratively while reducing time consumption and processing power to quickly achieve reliable results.[41,42]

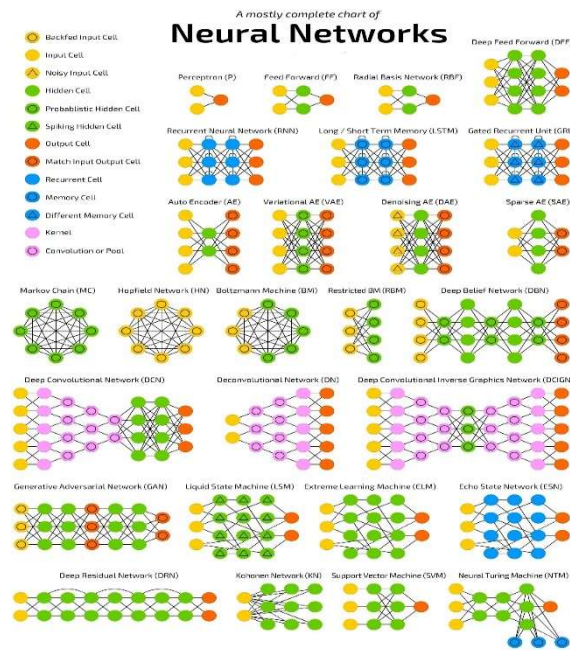


Figure 4.3: Types of Neural Networks (available to public domain [48])

Figure 4.3 pragmatically shows the different types of Neural Networks. For the sake of this study only Backpropagation Feed Forward Network will be discussed as it was found to be the most effective Regression model to predict the COP of the proposed DEAC System.

4.1.3. Backpropagation Neural Network [41, 42]:

The Backpropagation Learning Rule was discovered as early as 1974. It has been the network architecture of choice for a vast majority of applications. This because it has been extensively studied experimentally and theoretically.

There are two facets to the operation Backpropagation neural networks. The forward propagation of activation producing an output and the backward propagation of error which is essential for learning.

The Conventional BPNN Algorithm is trained through a 5-step process:

- Weights are assigned to the initial input values
- Feed Forward Operation using GDM (Gradient Descent Method)
- Backpropagation of errors using loss functions
- Adjustment of weights and biases to achieve desired outcome
- Optimization of Weights and Biases using Levenberg-Marquardt Method[49]

The input layer performs no processing and serves merely to disseminate the input values to the first processing layer. The layers maybe defined as i for input layer, h for hidden layer and o for output layer Where x_i denotes the input vector in the input layer. The summation function a in the hidden layer is the dot product of the weight vector w_i of the node with the x_i input vector. θ is the bias term for the node and n is the number of synapses for the node. Below Eqn shows the relationship as described:

$$a = \sum_{i=1}^n w_{ih}x_i + \theta \quad (13)$$

Next is the node output, which is determined from passing the net input of the node through the transfer function. A sigmoidal transfer activation function such as the one in the Eqn below is commonly used where o is the node output and a is the result of the summation function from the Eqn 13 above.

$$o = f(a_{ih}) = \frac{1.0}{1.0 + e^{-a}} \quad (14)$$

The above function is nonlinear in nature and it limits the values between 0 and 1. This normalization process avoids the domination effects of large input values and provides nonlinearity in the outputs.

The signal from the activation function is forwarded to the output layer

$$z_h = f(a_{ih}) \quad (15)$$

The signal z_h is multiplied by the weight of the hidden and output layer S_{ho}

$$a_{iho} = \sum S_{ho} z_h + c \quad (16)$$

This then becomes a function a_o represented as

$$a_o = f(a_{iho}) \quad (17)$$

The error function is generated after all the output nodes have received the processed input signal from the hidden layer where δ_o is the output unit error. The Eqn below describes the error function:

$$\delta_o = (b_o - a_o)f(a_{iho}) \quad (18)$$

In Backpropagation the unit error δ_o is sent back through the hidden layers, the Eqn describing this process. The repeated iteration of errors adjusts the weights and biases and minimizes the error which continues until the desired output is achieved. ΔS_{ho} is the difference function between the output error from the previous iteration and the resultant output error after being sent back into network through the hidden layers.

$$S_{ho}(new) = S_{ho}(old) + \Delta S_{ho} \quad (19)$$

ΔS_{ho} Is also defined as:

$$\Delta S_{ho} = \alpha \delta_o z_h \quad (20)$$

α Varies between 0 and 1

Another aspect to tackle in Machine Learning is Overfitting where a model learns the training data too well and captures noise or random fluctuations present in the data, rather than the underlying patterns. This can lead to poor generalization and reduced performance on new, unseen data.

In overfitting, a model becomes overly complex, fitting the training data's idiosyncrasies rather than learning the true relationships. As a result, it may exhibit high accuracy on the training data but struggle to perform well on validation or test data. Overfitting often occurs when a model is too flexible or when it's trained on too few data points relative to its complexity.

Key indicators of overfitting include:

1. Low Training Error, High Validation/Test Error: The model achieves very low error on the training data but performs poorly on validation or test data.
2. Large Model Complexity: Models with a large number of parameters, such as deep neural networks with many layers or high-degree polynomial regression, are prone to overfitting.

3. Memorization: The model starts to memorize the training data instead of learning general patterns, resulting in poor performance on new data.

To address overfitting, several strategies can be employed:

1. Regularization: Introduce penalties or constraints on the model's parameters during training to discourage overly complex solutions. Common regularization techniques include L1 and L2 regularization.

2. Cross-Validation: Divide the data into training, validation, and test sets. Cross-validation helps assess the model's performance on unseen data and select hyper parameters that lead to better generalization.

3. Early Stopping: Monitor the validation error during training and stop when it starts to increase, indicating that the model is beginning to overfit.

4. Feature Selection: Choose relevant features and remove irrelevant or redundant ones to simplify the model's complexity.

5. Reduce Model Complexity: Use simpler model architectures with fewer parameters to avoid capturing noise.

6. Data Augmentation: Introduce variations to the training data to provide the model with a more diverse set of examples.

7. Ensemble Methods: Combine predictions from multiple models to reduce overfitting by leveraging the wisdom of the crowd.

Overfitting is a crucial concern in machine learning, and striking a balance between model complexity and the amount of available data is key to achieving models that generalize well to new data.

4.1.4. Proposed Algorithm for prediction of COP:

The steps below were used to develop the architecture of the BPNN for this study:

1. Splitting the dataset for training, testing and validation in an optimal ratio with a majority of the data points being used to train the BPNN.
2. The Feature (Dimension) Selection to be used as inputs.

3. Number of Neurons in the Hidden Layer that are efficient and sufficient to produce the desired outcome.
4. Initialize random weights a_{ih}, S_{ho} , bias θ and minimum error δ_{omin} for priming the network.
5. Begin Training process by feeding the network with input data points for computation output and loss function.
6. The training should terminate when δ_{omin} becomes greater than δ_o . This will lock in the weights and biases.
7. When the Mean Squared Error converges to a value closest to 1 at that point the most accurate prediction will have been made. Below is the Eqn used to Calculate MSE:

$$MSE = \frac{1}{N} \sum_{i=1}^N (y_i - \hat{y}_i)^2 \quad (21)$$

Where N is the number of data points in the set?

y_i Is the actual target value for the i Th data point?

\hat{y}_i Is the prediction of BPNN for the i Th data point

8. The final step is to feed the BPNN novel data and use the prediction for validation with that of the actual output and theoretical output from EES model.[42,49]

Steps defining the Process of BPNN to Predict COP of DEAC System:

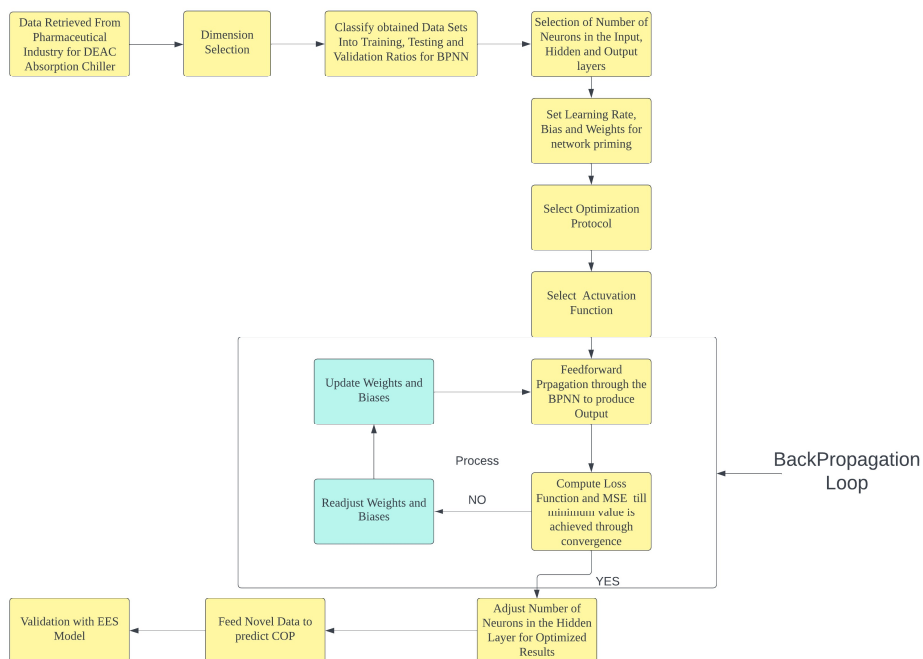


Figure 4.4: Process Flowchart of BPNN to Predict COP of DEAC System

Chapter 5. Results and Discussions

This chapter covers the Energy, Exergy, and Exergoeconomic Analysis of the Parallel Effect DEAC system. It also discusses the convergence and efficiency of the BPNN Machine Learning Model during training. Furthermore, a comparison between the EES model and the ML model has been made against the actual values

5.1. Energy, Exergy and Exergoeconomic analysis:

As discussed in chapter 3 the Mass, Energy and Exergy balance equations were outlined in the Table formed the basis of the EES model. Several assumptions were made as listed below to determine the values of enthalpies, Exergetic Efficiency and COP.

- All Calculations were done under steady state conditions. i.e., effects of Kinetic and Potential Energies were ignored.
- Pressure Loses and, in the pipelines, and all heat exchangers are negligible.
- Friction heat gain in the coils and impact of fouling have been ignored.
- Heat exchange between the system and surroundings with the exception of heat transfer at HG, Evaporator, Condenser-2 and Absorber does not occur.
- The reference ambient conditions at which T_o and P_o have been considered are 25 °C and 100 kPa.
- All Heat exchangers reject heat with the exception of the HG, to a water exchange loop.
- All state point condition assumptions have already been stated in Table __.
- Pumps are isentropic and have $\eta_p = 95\%$.
- The Burner Efficiency is taken at 85%.
- Both Solution Heat Exchangers have same effectiveness.
- Pressures changes only through Expansion Valves (which are also adiabatic) and Pumps.
- The outlet Temperatures from the absorber and from the two generators correspond to equilibrium conditions of mixing and separation.

The Table outlines the input values used for determination of the Enthalpies and subsequent Exergy calculation:

Table 6: input values used for determination of the Enthalpies and subsequent Exergy

Inputs		
Parameters	Denoted by Symbol	Value
Capacity	Q_e	1760 kW (500 Tons)
Evaporator Temperature	T_e	5 °C
Desorber Solution Exit Temperature	t_{14}	170 °C
Condenser-1/ LG Temperature	t_1, t_8	42.3 °C
Solution Heat Exchanger Effectiveness	ε	0.6
Mass flow rate of Chilled Water	m_{CHWR}	5035 kg/s
Gas Consumption Rate of DEAC	λ_{fuel}	165 Nm ³ /hr
Mass flow rate of Cooling Water	m_{Cwr}	4578 kg/s
Cooling Water Supply	T_{25}	32.2 °C
Cooling Water Return	T_{26}	37.8 °C
Chilled Water Supply	T_{27}	6 °C
Chilled Water Return	T_{28}	11°C

The following Table 7 and Table 8 shows the results retrieved from EES model which has calculated the both the Energy consumption as well as Exergy destruction of each component.

Table 7: EES model Energy calculation

State Points	h, (J/g)	Mass flow rate, (kg/s)	Temp, (°C)	Pre,(kPa)	X, % LiBr	S, (J/g °C)
0	358.5	-	40	101.6	-	1.143
1	120.2	9.55	42.4	0.89	-	0.2386
2	120.2	9.55	42.4	8.34	59.5	0.2386
3	184.6	9.55	75.6	8.34	59.5	0.4315
4	252.4	8.80	97.8	8.34	64.6	0.5149
5	177	8.80	58.8	8.34	64.6	0.3162
6	177	8.80	53.2	0.89	64.6	0.285
7	2659	0.32	85.7	8.34	0	8.456
8	177	0.75	42.4	8.34	0	0.6043
9	177	0.75	5.1	0.89	0	0.6388
10	2509	0.75	5.1	0.89	0	9.022
11	204.5	5.5	75.6	8.34	59.5	0.4878
12	204.5	5.5	75.6	111.8	59.5	0.4878
13	305.6	5.5	136.7	111.8	59.5	0.7533
14	385.5	5.1	170.7	111.8	64.6	0.8464
15	276.4	5.1	110.9	111.8	64.6	0.5783
16	276.4	5.1	99.1	0.89	64.6	0.5208
17	2787	0.43	155.7	111.8	0	7.587
18	431	0.43	102.8	111.8	0	1.339
19	431	0.43	42.4	0.89	0	0.6043
20	182	4.05	75.6	8.34	59.5	0.4048

Energy and Exergy Analysis of Components in DEAC:

Table 8: EES Model Exergy calculations

Parameters	Symbol	Energy (kW)	Symbol	Exergy Destruction kJ/kg
Absorber	Q_a	2333	$\dot{E}x_{dest,a}$	1931
Solution Pump-1	W_p	negligible	$\dot{E}x_{dest,p}$	negligible
LTX (Low Temperature Heat Exchanger)	-	-	$\dot{E}x_{dest,LTX}$	11.34
LG (Low Pressure Generator)	Q_{LG}	1022	$\dot{E}x_{dest,LG}$	79.18
Solution Pump-2	W_{p2}	negligible	$\dot{E}x_{dest,p2}$	negligible
HTX (High Temperature Heat Exchanger)	-	3091	$\dot{E}x_{dest,HTX}$	4.497
HG (High Pressure Generator)	Q_{HG}	1484	$\dot{E}x_{th,HG}$	2471
Condenser-2	Q_{cd2}	1022	$\dot{E}x_{dest,CD2}$	984.7
Condenser-1	Q_{cd1}	904	$\dot{E}x_{dest,CD1}$	602.6
Evaporator	Q_e	1760	$\dot{E}x_{dest,E}$	122.47
Solution Expansion Valve-1	-	-	$\dot{E}x_{dest,SEV,1}$	negligible
Solution Expansion Valve-2	-	-	$\dot{E}x_{dest,SEV,2}$	negligible
Refrigerant Expansion Valve-1	-	-	$\dot{E}x_{dest,REV,1}$	negligible
Refrigerant Expansion Valve-2	-	-	$\dot{E}x_{dest,REV,2}$	negligible

As can be observed from the above Table, the highest exergy destruction takes place in the HG which is almost 30% higher than the Exergy destruction in the Absorber. Together, the highest exergy destruction takes place in the High Temperature Generator and the Absorber making up 70% of the total exergy destruction. These results agree with those studies that have been discussed at length in Chapter 2.

Crucially, the major value we sought after was the COP of the DEAC which came out to be 1.18. The work energy of pumps was considered to be negligible when compared to Heat Input of the Generator.

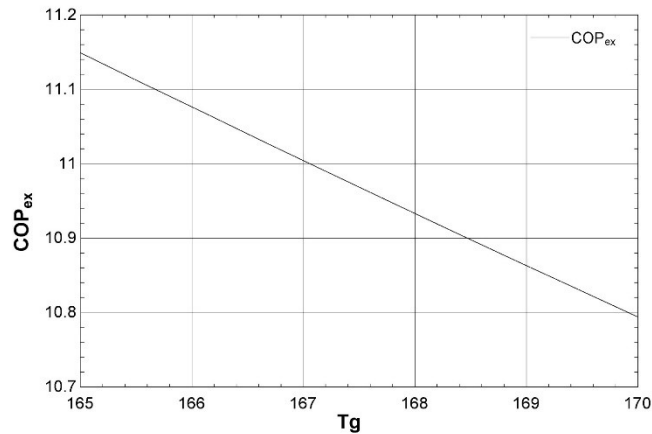


Figure 5.1: T_g vs Exergetic Efficiency

The above Figure illustrates the negative trend of reduction of Exergetic Efficiency with respect to increasing the Generator Temperature. This is because the limiting factor is the size of heat exchanger which remains the same. Therefore, as higher heat input is unable to be transferred to the cycle the exergetic efficiency decreases.

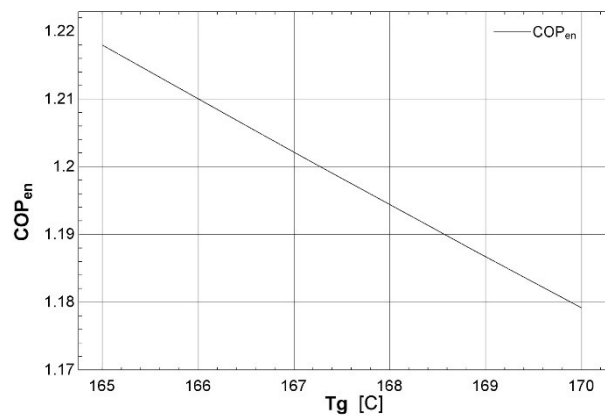


Figure 5.2: T_g vs COP

Again the same trend can be seen as previously seen, the energy efficiency decreases as well due to the size of the heat exchanger remaining the same. Likewise all other parameter such as exergy destruction follow suit in the same trend.

5.2. Exergoeconomic Analysis:

It is imperative to understand the Exergoeconomic aspect of the DEAC system. Below is the Total Equipment Cost, Operation and Maintenance Cost and Cost of Cooling per kW

Using the Equations from Chapter 3, the following calculation yielded the result:

$$\dot{Z}_{eq}(\$) = 1144.3 (1760)^{0.67}$$

Hence the Total Cost of the proposed DEAC is approximately, $\dot{Z}_{eq} = \$171,000$.

The operation and maintenance cost is 3% of the Total Cost of DEAC, $\dot{C}_{OPM} = \$5130$

The Exergetic Cost of Cooling is then computed to be

$$c_{cool} = \frac{171000 + 5130}{122.47} = 1435.45 \$/kW$$

The Exergetic Cost of Cooling comes out to be approximately 1435.45 $\$/kW$. As per general market dynamics, this value is similar to most DEAC systems being installed in Pakistan.

BPNN to predict the COP of DEAC System:

The main focus of this study was to validate the EES model with that of the ANN Model and Real World Data. The real world data was obtained from a Pharmaceutical Plant whereby the tolerance for Chilled Water Supply temperature was only 1° C. Effectively there wasn't much variance in the Cooling Load due to the tolerance restriction. The reason behind this was that the Chilled Water requirement was not required for space cooling but instead was required for Process Cooling in Gel Manufacturing Department.

However, variations in the Cooling Water Temperature are were possible due to changes in the performance of the Cooling Tower which in turn is heavily dependent on the wet bulb temperature of the Ambient Environment. Changes in Gas Consumption rate were also needed to be considered due to inconsistencies in Natural Gas Supply Pressures this changes the Heat Input Rate into the High Temperature Generator Range.

It is important to note that the Data was acquired through the Absorption Chillers HMI (Human-Machine Interface) logic control system. The Dataset range was of 6 months from October 2020 till June 2021. Data for the period of November 2020, December 2020 and January 2020 was not available due to Plant Maintenance shut down during this period. The 6 Input parameters that influence the the DEACs' COP the most are listed as follows:

1. Chilled Water Supply Temperature
2. Chilled Water Return Temperature
3. Cooling Water Supply Temperature
4. Cooling Water Return Temperature
5. High Generator Temperature
6. Gas Consumption Rate

The data was divided into 70: 15:15 ratio which effectively translates to 5 months required for Training and Testing and 1 months' worth of data for Validation or predictions. There were too many data points in these 6 Feature sets because the Chiller operation was of 24 hours and there was hourly data. Therefore, daily averages of the dataset were taken to reduce the data points to 181. This would result in less computational power required during training as well as reduce time consumption and risk of noise or over fitting.

The entire process of training the BPNN was iterative. MATLAB ANN App tool were an effective way to model the DEAC system. The Feed Forward Back Propagation option was used and LM was used to optimize the error function.

The iterative process required tweaking various aspects such as the number of neurons in layer, readjustment of weights and biases, alter learning rate and other aspects, although only the mentioned three facets were changed.

The neurons were changed in increments of 10. The best result was recorded at 20 neurons. The below diagram shows the pictorial model of the BPNN architecture which was 6-20-1.

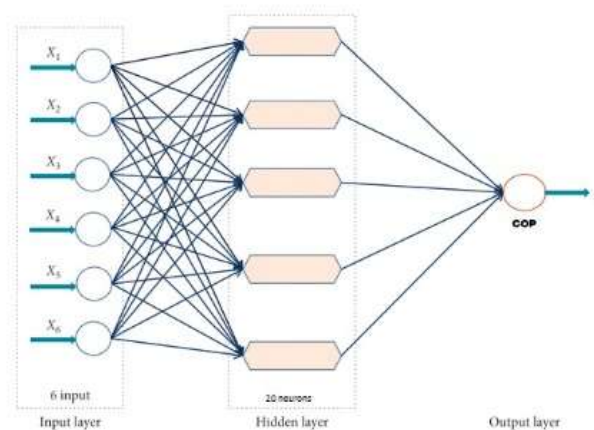


Figure 5.3: Optimal Neural Network Architecture for COP Prediction of DEAC (Adapted from [28])

In each iteration, weights and biases were initialized over an input range. The 6 input features produce an input signal and are assigned the weights and biases in the hidden layer containing the selected number of neurons. Conversely, an error is calculated of the loss function. The error is backpropagated through the hidden layer. The sigmoidal transfer functions uses LM to optimize the output signal all while reducing the error rate every time back propagation is done. The number of cycles where the most reliable value of R^2 is reached after which no more convergence is possible is known as Epoch.

Table 9: Results of Iterations Summarized

S.No.	Neurons in hidden layer	MSE	No. of epochs	R^2 value - Training	R^2 value - Validation	R^2 value - Testing	R^2 value - Overall
1	10	0.0361289	660	0.99998	1	0.99988	0.99995
2	20	0.000106056	19	1	1	1	1
3	30	0.0056134	100	1	1	1	1
4	40	0.0005873	50	1	1	1	1
5	50	0.041425	7	1	1	1	1
6	60	0.116241	1000	0.99896	0.99177	0.99382	0.99516
7	70	1.002346	37	0.99999	0.99977	0.997657	0.99897
8	80	5.1832	500	0.99979	0.98992	0.99919	0.99465
9	90	133.2475	28	0.99993	0.99991	0.95897	0.99750
10	100	8000.6393	1	0.705832	0.894034	0.61567	0.70434

The above table represents the iterative runs that were done in increments of 10 neurons. We can observe from the table above that as the number of parameters as mentioned previously are tweaked as well as with the increase in the number of neurons the value of R reaches closer and closer to 1 only upto a certain point after which the both the MSE and R^2 value become divergent. Which means the correlation between the predicted output data and target becomes stronger only till a certain point until overfitting increases the backpropagated errors and divergence causes reduction in the output accuracy.

However, the best performance observed where $R = 1$ was at 20 neurons and MSE 0.00016056 as can be seen from the Figures below. The predicted output dataset in the testing, training and validation charts show convergence towards the regression line.

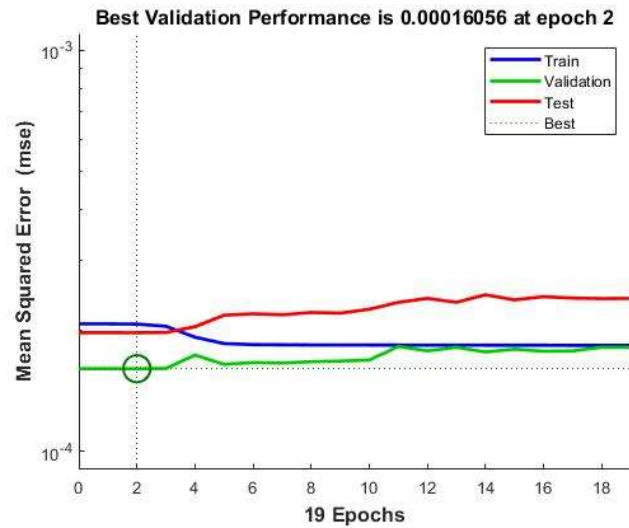


Figure: Mean Squared Error at best validation performance

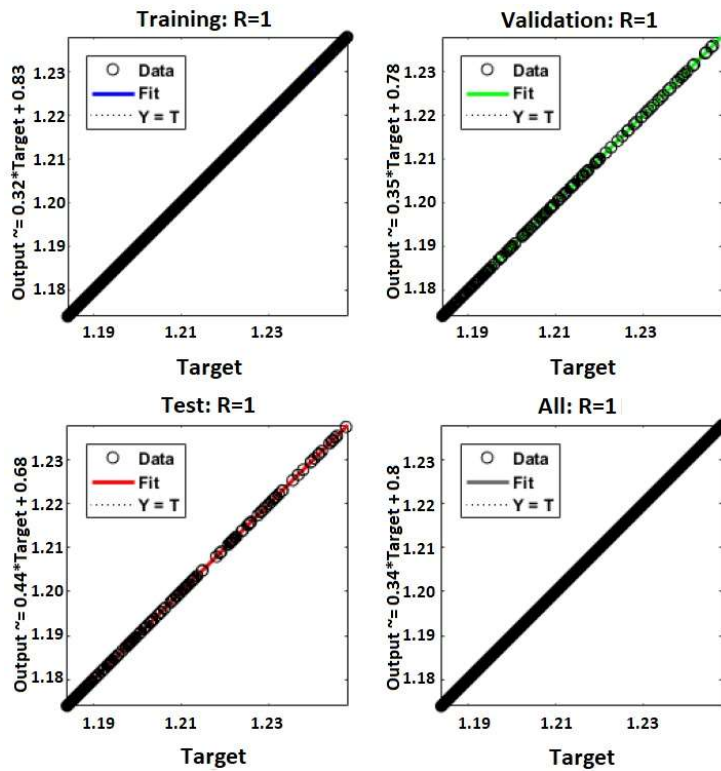


Figure: R value at best validation performance

5.3. Validation of Predictive Results with EES Mode and Actual Values

After the BPNN model was trained, When R=1, the input values used for modelling of EES while in the steady state were T₂₅, T₂₆, T₂₇ and T₂₈ temperatures which were actually Chilled Water and Cooling water Supply and Return temperatures.

Table 10: COP Comparison of Actual vs. ANN model vs. EES model

Actual COP	Predicted COP	EES Model COP
1.12	1.18	1.18

Table 10 illustrates the results of the two models ANN and EES versus the actual COP which shows a slight difference. This could be due to the fact that the OEM provided COP takes into account a plethora of factors such as variations in Ambient Temperatures, Vacuum Losses, Fouling Effects, and Degradation of HEX Coils etc.

Chapter 6. Conclusion & Future Work

6.1. Conclusion

To sum up, this study focused on covering the key objectives as outlined which was to carry out an Energy, Exergy and Exergoeconomic analysis of the Parallel flow DEAC system, Develop an AI based data driven model to predict the COP of the proposed DEAC system and Finally validate the results with the actual COP and the COP calculated from the thermodynamic simulation.

The EES model was developed using classical mass, energy and exergy balance equations. Several assumptions were made and outlined in order to generate viable values from the thermodynamic model. The results reinforced the past studies and also validated the performance of this study's model in that the Exergy destruction was found to be the highest in the High Temperature Generator. Moreover the Exergy destruction from the Absorber and HG accounted for 70% of the total Exergy destruction of the system. Finally, the COP and Exergetic Efficiency were also computed in the steady state condition. The results showed that the Higher the Temperature of the High pressure generator, the lower the COP and Exergetic Efficiency due to the fixed size of the Heat Exchanger. Furthermore, the Exergoeconomic analysis revealed the Cost of Cooling in USD per kW was within market norms.

In the second part of this report, various ANN models were studied and it was concluded to proceed with Backpropagation Neural Network or BPNN with Levenberg-Marquardt Optimization technique for predicting the COP of the parallel flow DEAC system. The feature selection for the input values of the model was done based on the most influential and easily available parameters such as the Chilled Water and Cooling Water Supply and Return Temperatures in addition to the High Pressure Generator Temperature and Gas Consumption Rate. The BPNN model was trained with 70% percent of the sample dataset, tested with 15%

of the sample dataset and finally validated with the remaining 15%. The iterative process of changing neurons, readjustment of weights and biases and altering the learning rate was time consuming but fruitful. The best variation of the BPNN model was deduced from the various iteration as having MSE of 0.00016056 at 19 Epochs with a network architecture of 6-20-1. Also the R value converged at 1 indicating a strong correlation between the target value and the predicted output value.

Finally, the COP of the EES model, Actual COP and Predicted COP were in close agreement to each other and the reason for their differences were discussed. Hence, we can confidently hypothesize that ANN and Machine Learning models can correlate Non Linear data without the use of complex empirical and/or thermodynamic models by using complex statistical and intelligent algorithms, which themselves are developing day by day based on the use case and efficacy of the system. Additionally, thermodynamic models require the use of assumptions which leads to oversimplification especially in the case of Non-Steady Systems.

6.2. Future Work

The application of machine learning in the field of absorption chillers holds several promising avenues for future research and development. Some potential areas of future work include:

1. **Advanced Control Strategies:** Machine learning can be used to develop more advanced and adaptive control strategies for absorption chillers. These strategies could optimize the operation of the chiller system in real-time, considering variables like ambient conditions, load demand, and energy costs.
2. **Fault Detection and Diagnostics:** Machine learning algorithms can be employed to detect and diagnose faults in absorption chiller systems. This would enable early identification of issues and facilitate proactive maintenance, improving overall system reliability and efficiency.
3. **Optimal Sizing and Configuration:** Machine learning techniques can aid in determining the optimal sizing and configuration of absorption chiller systems based on specific application requirements and constraints. This could lead to more efficient and cost-effective designs.
4. **Predictive Maintenance:** Using historical data and sensor information, machine learning models can predict when maintenance is likely to be required, minimizing downtime and reducing maintenance costs.
5. **Integration with Renewable Energy Sources:** Absorption chillers can be integrated with renewable energy sources like solar or waste heat. Machine learning algorithms can help

optimize the operation of these hybrid systems to make the most efficient use of available energy sources.

6. Energy Demand Forecasting: Machine learning can contribute to accurate forecasting of energy demand, allowing absorption chiller systems to proactively adjust their operation to meet varying loads and optimize energy consumption.

7. Efficiency Improvement: Machine learning algorithms can be applied to optimize heat and mass transfer processes within absorption chillers, potentially leading to improved overall efficiency.

8. Multi-Objective Optimization: Machine learning can assist in finding trade-offs between various performance metrics such as Coefficient of Performance (COP), energy consumption, and environmental impact, leading to more sustainable design and operation.

9. Hybrid Models: Combining physics-based models with machine learning approaches can create hybrid models that leverage the strengths of both approaches for more accurate predictions and system optimization.

10. Data-Driven Insights: Machine learning can uncover insights from large datasets that might not be apparent through traditional analysis, contributing to a deeper understanding of absorption chiller behavior and performance.

11. Real-time Decision Support: Implementing machine learning in real-time decision support systems can aid operators in making optimal decisions for chiller system operation.

12. Lifecycle Analysis and Optimization: Machine learning can assist in performing lifecycle analysis of absorption chiller systems, optimizing their design, operation, and retirement phases for maximum efficiency and sustainability.

In summary, the future of machine learning in absorption chillers lies in creating smarter, more adaptive, and efficient systems through advanced control, diagnostics, optimization, and integration with emerging technologies.

Chapter 7. References

- [1] Westphalen, D., & Koszalinski, S. (2001). Energy consumption characteristics of commercial building hvac systems volume I: Chillers, refrigerant compressors, and heating systems. Final Report to the Department of Energy (Contract No. DE-AC01-96CE23798).
- [2] Maximize Market Research. (Year, Month Day of publication not provided). *Absorption ChillersMarket*.MaximizeMarketResearch.URL:
<https://www.maximizemarketresearch.com/market-report/absorption-chillers-market/188814/>
- [3] PS Market Research. (Year, Month Day of publication not provided). HVAC Market. PS Market Research. URL: <https://www.psmarketresearch.com/market-analysis/hvac-market/>
- [4] Yahoo Finance. (Year, Month Day of publication not provided). Global Absorption Chillers Market Report. Yahoo Finance. URL: <https://finance.yahoo.com/news/global-absorption-chillers-market-report-130300555.html>
- [5] Lu, M., & Lai, J. H. (2019). Building energy: a review on consumptions, policies, rating schemes and standards. *Energy Procedia*, 158, 3633-3638.
- [6] Adhikari, S., & Gordy, P. (2022). Energy and Cost Comparison of Building Cooling Systems. *EPiC Series in Built Environment*, 3, 731-739.
- [7] “Electricity – Global Energy Review 2021 – Analysis - IEA.” [Online]. Available: <https://www.iea.org/reports/global-energy-review-2021/electricity>. [Accessed: 23-Mar-2022].
- [8] Kistler, P., & NAVAL FACILITIES ENGINEERING SERVICE CENTER PORT HUENEME CA. (1997). Advantages and Disadvantages of Using Absorption Chillers to Lower Utility Bills. *California: Naval Facilities Engineering Service Center*.
- [9] Verified Market Research. (Year, Month Day of publication not provided). Absorption Chiller Market. Verified Market Research. URL:
<https://www.verifiedmarketresearch.com/product/absorption-chiller-market/>
- [10] Nikbakhti, R., Wang, X., Hussein, A. K., & Iranmanesh, A. (2020). Absorption cooling systems–Review of various techniques for energy performance enhancement. *Alexandria Engineering Journal*, 59(2), 707-738.

- [11] Čongradac, V., & Kulić, F. (2012). Recognition of the importance of using artificial neural networks and genetic algorithms to optimize chiller operation. *Energy and Buildings*, 47, 651-658.
- [12] Mohanraj, M., Jayaraj, S., & Muraleedharan, C. (2012). Applications of artificial neural networks for refrigeration, air-conditioning and heat pump systems—A review. *Renewable and sustainable energy reviews*, 16(2), 1340-1358.
- [13] Puig-Arnavat, M., López-Villada, J., Bruno, J. C., & Coronas, A. (2010). Analysis and parameter identification for characteristic equations of single-and double-effect absorption chillers by means of multivariable regression. *International journal of refrigeration*, 33(1), 70-78.
- [14] Gomri, R. (2009). Second law comparison of single effect and double effect vapour absorption refrigeration systems. *Energy Conversion and Management*, 50(5), 1279-1287.
- [15] Gomri, R., & Hakimi, R. (2008). Second law analysis of double effect vapour absorption cooler system. *Energy conversion and management*, 49(11), 3343-3348.
- [16] Labus, J., Bruno, J. C., & Coronas, A. (2013). Performance analysis of small capacity absorption chillers by using different modeling methods. *Applied Thermal Engineering*, 58(1-2), 305-313.
- [17] M. Izquierdo, J. D. Marcos, M. E. Palacios, and A. Gonzalez-Gil, "Experimental evaluation of a low-power direct air-cooled double-effect LiBr-H₂O absorption prototype," *Energy*, vol. 37, pp. 737-748, 2012.
- [18] H.J. Manohar, R. Saravanan, & S. Renganarayanan. (2006). Modelling of steam fired double effect vapour absorption chiller using neural network. *Energy Conversion and Management*, 47(15–16), 2202-2210. ISSN 0196-8904.
- [19] Md. Azhar & M. Altamush Siddiqui. (2020). Comprehensive exergy analysis and optimization of operating parameters for double effect parallel flow absorption refrigeration Cycle. *Thermal Science and Engineering Progress*, 16, 100464. ISSN 2451-9049.
- [20] Hu, Y., Schaefer, L., & Hartkopf, V. (2011). Energy and exergy analysis of double effect (parallel and series flow) absorption chiller systems. In *Proceedings of the 10th International Conference on Heat Power Plants (Order No. HPP-CONF10)*. September 20, 2011.

- [21] Kaynakli, O., Saka, K., & Kaynakli, F. (2015). Energy and exergy analysis of a double effect absorption refrigeration system based on different heat sources. *Energy Conversion and Management*, 106, 21-30. ISSN 0196-8904.
- [22] Kaushik, S.C., & Arora, A. (2009). Energy and exergy analysis of single effect and series flow double effect water–lithium bromide absorption refrigeration systems. *International Journal of Refrigeration*, 32(6), 1247-1258. ISSN 0140-7007.
- [23] Azhar, Md., & Siddiqui, M. A. (2017). Energy and exergy analyses for optimization of the operating temperatures in double effect absorption cycle. *Energy Procedia*, 109, 211-218. ISSN 1876-6102.
- [24] Shirmohammadi, S.M.S. Mahmoudi, and M.A. Rosen. The paper was published in the journal "Applied Thermal Engineering," in Volume 152, in the year 2019, on pages 643-653. The ISSN (International Standard Serial Number) for the journal is 1359-4311.
- [25] Kovacı, T., & Şahin, A. Ş. (2018). Energy and exergy analysis of a double-effect LiBr-H₂O absorption refrigeration system. *International Journal of Energy and Environment*, 9(1), 37-48.
- [26] Chow, K. W., Zang, Y., & Son, Y. "Global Optimization of Absorption Chiller Using Genetic Algorithm." *IEEE Transactions on Sustainable Energy*, vol. 8, no. 4, pp. 1786-1794, 2017.
- [27] Park, S., Ahn, K. U., Hwang, S., Choi, S., & Park, C. S. (2019). Machine learning vs. hybrid machine learning model for optimal operation of a chiller. *Science and Technology for the Built Environment*, 25(2), 209-220.
- [28] Chahartaghi, M., Golmohammadi, H., & Shojaei, A. F. (2019). Performance analysis and optimization of new double effect lithium bromide–water absorption chiller with series and parallel flows. *International Journal of Refrigeration*, 97, 73-87.
- [29] Feierl, L., Innerhofer, P., Poier, H., Moser, M., & Holter, C. (2019). Artificial Neural Network for performance prediction of Absorption Chillers of Large-Scale Solar-Air-Conditioning Systems.
- [29] Kim, J. H., Seong, N. C., & Choi, W. (2020). Forecasting the energy consumption of an actual air handling unit and absorption chiller using ANN models. *Energies*, 13(17), 4361.
- [30] Tian, C., Wang, Y., Ma, X., Chen, Z., & Xue, H. (2021). Chiller Fault Diagnosis Based on Automatic Machine Learning. *Frontiers in Energy Research*, 9, 753732.

- [31] Myat, A., Thu, K., Kim, Y. D., Chakraborty, A., Chun, W. G., & Ng, K. C. (2011). A second law analysis and entropy generation minimization of an absorption chiller. *Applied thermal engineering*, 31(14-15), 2405-2413.
- [32] Lubis, A., Jeong, J., Giannetti, N., Yamaguchi, S., Saito, K., Yabase, H., & Alhamid, M. I. (2018). Operation performance enhancement of single-double-effect absorption chiller. *Applied energy*, 219, 299-311.
- [33] Kim, J. H., Seong, N. C., & Choi, W. C. (2021). Comparative Evaluation of Predicting Energy Consumption of Absorption Heat Pump with Multilayer Shallow Neural Network Training Algorithms. *Buildings*, 12(1), 13.
- [34] Xu, Z. Y., Wang, R. Z., & Xia, Z. Z. (2013). A novel variable effect LiBr-water absorption refrigeration cycle. *Energy*, 60, 457-463.
- [35] Aisyah, N., Alhamid, M. I., Saha, B. B., Sholahudin, S., & Lubis, A. (2019). Solar absorption chiller performance prediction based on the selection of principal component analysis. *Case Studies in Thermal Engineering*, 13, 100391.
- [36] M. Barthwal, A. Dhar, and S. Powar, "The Techno-Economic and Environmental Analysis of Genetic Algorithm (GA) Optimized Cold Thermal Energy Storage (CTES) for Air-Conditioning Applications," *Appl. Energ.*, vol. 283, p. 116253, 2020. [Online]. Available: doi: 10.1016/j.apenergy.2020.116253.
- [37] Hu, J., Teng, K., Qiu, Y., Chen, Y., Wang, J., & Lund, P. (2022). Thermodynamic and Economic Performance Assessment of Double-Effect Absorption Chiller Systems with Series and Parallel Connections. *Energies*, 15(23), 9105.
- [38] Taye, M. M. (2023). Understanding of Machine Learning with Deep Learning: Architectures, Workflow, Applications and Future Directions. *Computers*, 12(5), 91.
- [39] Fathalla, Eissa & Tanaka, Yasushi & Maekawa, Koichi. (2018). Remaining fatigue life assessment of in-service road bridge decks based upon artificial neural networks. *Engineering Structures*. 171. 10.1016/j.engstruct.2018.05.122.
- [40] Buscema, M. (2002). A brief overview and introduction to artificial neural networks. *Substance use & misuse*, 37(8-10), 1093-1148.
- [41] Shanmuganathan, S., & Samarasinghe, S. (Eds.). (Year of Publication). *Artificial Neural Network Modelling* (Volume 628 of *Studies in Computational Intelligence*). Springer.

- [42] Papakyriakou, D., & Barbounakis, I. S. (2022). Data mining methods: a review. *International Journal of Computer Application*, 183(48), 5-19.
- [43] Han, S. H., Kim, K. W., Kim, S., & Youn, Y. C. (2018). Artificial neural network: understanding the basic concepts without mathematics. *Dementia and Neurocognitive Disorders*, 17(3), 83-89.
- [44] Hounmenou, C. G., Gneyou, K. E., & KAKAI, R. L. G. (2021). A Formalism of the General Mathematical Expression of Multilayer Perceptron Neural Networks.
- [45] WordStream. (2017, July 28). Machine Learning Applications: 10 Companies Using Machine Learning. WordStream. Retrieved August 19, 2023, from <http://www.wordstream.com/blog/ws/2017/07/28/machine-learning-applications>
- [46] IBM Developer. (Year, Month Day). What Is Automated AI for Decision Making?. IBM Developer. Retrieved August 19, 2023, from <https://developer.ibm.com/learningpaths/get-started-automated-ai-for-decision-making-api/what-is-automated-ai-for-decision-making/>
- [47] G2 Learning Hub. Title of the webpage. G2 Learning Hub. Retrieved August 19, 2023, from <https://learn.g2.com/artificial-neural-network>
- [48] Jain, A. K., Mao, J., Mohiuddin, K.M., & ZBMAZmaden Research Center. (1996). Artificial Neural Network: A Tutorial. Michigan State University.
- [49] The Mostly Complete Chart of Neural Networks, Explained. Towards Data Science. Retrieved August 19, 2023, from <https://towardsdatascience.com/the-mostly-complete-chart-of-neural-networks-explained-3fb6f2367464>